DOI: 10.1534/genetics.106.061283

A Gain-of-Function Screen Identifying Genes Required for Vein Formation in the *Drosophila melanogaster* Wing

Cristina Molnar, Ana López-Varea, Rosario Hernández and Jose F. de Celis[1]

Centro de Biología Molecular "Severo Ochoa," Universidad Autónoma de Madrid, 28049 Madrid, Spain

Manuscript received May 24, 2006
Accepted for publication August 21, 2006

ABSTRACT

The formation of the Drosophila wing involves developmental processes such as cell proliferation, pattern formation, and cell differentiation that are common to all multicellular organisms. The genes controlling these cellular behaviors are conserved throughout the animal kingdom, and the genetic analysis of wing development has been instrumental in their identification and functional characterization. The wing is a postembryonic structure, and most loss-of-function mutations are lethal in homozygous flies before metamorphosis. In this manner, loss-of-function genetic screens aiming to identify genes affecting wing formation have not been systematically utilized. As an alternative, a number of genetic searches have utilized the phenotypic consequences of gene gain-of-expression, as a method more efficient to search for genes required during imaginal development. Here we present the results of a gain-of-function screen designed to identify genes involved in the formation of the wing veins. We generated 13,000 P-GS insertions of a *P* element containing UAS sequences (P-GS) and combined them with a Gal4 driver expressed mainly in the developing pupal veins. We selected 500 P-GSs that, in combination with the Gal4 driver, result in modifications of the veins, changes in the morphology of the wing, or defects in the differentiation of the trichomes. The *P*-element insertion sites were mapped to the genomic sequence, identifying 373 gene candidates to participate in wing morphogenesis and vein formation.

GENETIC screens have been instrumental in the identification of the molecules involved in controlling developmental processes in a variety of model organisms. The underlying assumption of most screens is that loss-of-function phenotypes identify the functional requirements of the affected gene and, at the same time, reveal the genetic logic of the biological process under consideration. There are many examples of the power conferred by well-designed mutagenic screens to dissect complex biological processes, using organisms as diverse as bacteria, yeast, *Caenorhabditis elegans*, *Arabidopsis thaliana*, Drosophila, and some vertebrates. Classic examples of loss-of-function genetic screens are those aiming to identify the genes controlling the progression through the cell cycle in yeast (Verde *et al.* 1995), the onset of cell death in *C. elegans* (Kinchen and Hengartner 2005), and the genetic circuitry involved in Drosophila embryonic segmentation (Nusslein-Volhard *et al.* 1984; Schupbach and Wieschaus 1986). With the availability of new techniques to manipulate and monitor gene expression, the search for genes affecting particular developmental processes has resulted in a wealth of information (Brand and Perrimon 1993; Nybakken *et al.* 2005).

[1]*Corresponding author:* Centro de Biología Molecular "Severo Ochoa," Universidad Autónoma de Madrid, Cantoblanco, 28049 Madrid, Spain. E-mail: jfdecelis@cbm.uam.es

The development of the veins in the Drosophila wing is a convenient system to analyze pattern formation mechanisms, cell differentiation, and the regulation of the activity of signaling pathways (de Celis 2003). The veins are formed by rows of cells that differentiate heavily pigmented cuticle and smaller apical size compared to the interveins. The patterning of veins involves the establishment of proveins and interveins in the wing disc, in a process regulated by the Hedgehog and Decapentaplegic signaling pathways (Bier 2000; de Celis 2003). These pathways define the expression of several transcription factors involved in the partition of the wing disc epithelium into provein and interveins. Subsequently, the expression of several members of the EGFR and Notch signaling pathways is activated within the proveins, leading to the subdivision of each provein in a central region that will differentiate as vein, where EGFR signaling is active, and two adjacent rows of boundary provein cells where Notch signaling prevents vein differentiation (Bier 2000; de Celis 2003). During metamorphosis the expression of *dpp* is activated in the developing veins, and its signaling pathway contributes to vein differentiation (de Celis 1997; Bier 2000). In this manner, the formation of veins in the correct place, and with a characteristic width, depends on the activity of well-conserved signaling pathways. All these characteristics make wing vein formation a suitable system to analyze the interactions between signaling pathways and

the regulation by their activities of cellular differentiation. Furthermore, changes in the vein pattern, including those caused by inappropriate activity of the key signaling pathways, are easily detected under the dissecting microscope, facilitating the isolation of mutations affecting vein formation (Diaz-Benjumea and Garcia-Bellido 1990).

A difficulty in designing genetic screens to identify the elements participating in wing patterning is that most amorphic alleles are lethal in homozygosis (Ripoll and Garcia-Bellido 1973; Diaz-Benjumea and Garcia-Bellido 1990). Approximately 90% of lethal alleles can be studied in mitotic recombination clones, because they are cell viable (Ripoll and Garcia-Bellido 1973). However, this requires the generation of mosaics, which generally involves several generations of crosses (Garcia-Bellido and Dapena 1974). The use of FRT-based mitotic recombination (Golic 1991) coupled with Gal4/UAS-FLP (Brand and Perrimon 1993) has overcome this difficulty by allowing the generation of cells homozygous for a lethal allele in an otherwise heterozygous individual (Xu and Rubin 1993; Babcock *et al.* 2003; Janody *et al.* 2004). However, the mutagenic agents used in such screenings, such as ethyl methanesulfonate (EMS), produce small alterations in the DNA sequence that are time-consuming to map, complicating the assignation of the mutants to the affected genes (Zipperlen *et al.* 2005). Therefore, the use of chemical mutagenesis to isolate genes involved in adult patterning has been of limited efficiency. An alternative that has been more widely employed relies on analyzing the phenotypic consequences of the ectopic and/or increased expression of genes in a particular tissue of interest. It has been generally observed that this manipulation of gene expression results in phenotypes that are informative about the normal function of the gene and might uncover genes that, due to functional redundancy, are not easily found in loss-of-function screens (for example, see Brand and Perrimon 1993; Sotillos and De Celis 2005). Furthermore, coupling UAS sequences to a P-transposable element allows targeting the expression of a considerable fraction of the genome to the tissues where the Gal4 protein is present. In general, gain-of-function screens using P-UAS elements consist of the analysis of the phenotypes resulting from the combination of a previously established collection of P-UASs and a Gal4 line expressed in the tissue of interest (Abdelilah-Seyfried *et al.* 2000; Pena-Rangel *et al.* 2002; Tseng and Hariharan 2002; Schulz *et al.* 2004). These screens have also been adapted to identify modifiers of particular signaling pathways (Brumby *et al.* 2004; Hall *et al.* 2004; Raymond *et al.* 2004; Zhu *et al.* 2005).

In this work we present the results of a gain-of-function screen aiming to identify genes involved in vein formation. We used a Gal4 driver expressed mainly in the developing pupal veins (*Gal4-shv^{3Kpn}*; Sotillos and de Celis 2006) and combined it with newly generated insertions of a *P* element containing UAS sequences (P-GS) (Toba *et al.* 1999). Among 13,000 new P-GS insertions we isolated 500 that cause alterations in the differentiation of the veins and/or the general morphology of the wing. The molecular mapping of the *P*-element insertion sites identifies 245 sites with 373 candidate genes, including ~60% of the known genes belonging to the Notch, EGFR, and Dpp signaling pathways.

MATERIALS AND METHODS

Drosophila stocks: We used the following stocks: *y w; Δ2-3 Dr/TM2*; *w; CyO P-GS/If*; the Gal4 lines *Gal4-1348*, *Gal4-sal*, *Gal4-vg^{DV}*, *Gal4-638*, *Gal4-shv^{3Kpn}* (Sotillos and de Celis 2006), and *Gal4-253*; and the UAS lines *UAS-GFP* (Ito *et al.* 1997), *UAS-N^{ecd}* (Lawrence *et al.* 2000), *UAS-rho* and *UAS-Ni* (de Celis *et al.* 1997), *UAS-dad* (Tsuneizumi *et al.* 1997), *UAS-brk* (Minami *et al.* 1999), *UAS-dpp* (Staehling-Hampton and Hoffmann 1994), *UAS-dpp-GFP* (Teleman and Cohen 2000), *UAS-tkv^{QD}* (Nellen *et al.* 1996), *UAS-EGFR*, *UAS-EGFR^{DN}*, *UAS-ras^{V12}* (Buff *et al.* 1998), *UAS-h*, *UAS-shn* (Marty *et al.* 2000), *UAS-Med* (Marquez *et al.* 2001), *UAS-Mef2* (Bour *et al.* 1995), *UAS-apt* (Eulenberg and Schuh 1997), *UAS-hh* (Ingham and Fietz 1995), *UAS-Dl* (Huppert *et al.* 1997), *UAS-N* (Lawrence *et al.* 2000), *UAS-yrt* (this work), and *UAS-CG11617* (a gift from Luis M. Escudero). Unless otherwise stated, crosses were done at 25°. Wings were mounted in lactic acid:ethanol (1:1) and photographed with a Spot digital camera and a Zeiss Axioplan microscope. Lines not described in the text can be found in FlyBase (Gelbart *et al.* 1997).

Generation of new P-GS insertions: We used *Δ2-3* (Robertson *et al.* 1988) as a source of transposase to mobilize a P-GS element placed in a CyO chromosome in a w^- background (Figure 1E). Males carrying both *CyO, P-GS* and *Δ2-3* were crossed with homozygous w females. The w^+ CyO^+ progeny was crossed in groups of 5–10 w^+ individuals with *Gal4-shv^{3Kpn}* flies, and the progeny of these crosses was scored to identify wing phenotypes. Individual stocks were established using the stock *w; CyO/If; Gal4-shv^{3Kpn}/TM2* (see Figure 1F for a summary of the crosses). The *Gal4-shv^{3Kpn}* driver (Figure 1D) is expressed mainly in the developing veins from 6 hr after puparium formation (APF). This expression is detected at least until 40 hr APF (Figure 1, A–C). Weak levels of Gal4 expression are also observed in the pupal interveins from 8 until 30 hr APF (Sotillos and de Celis 2006).

Molecular mapping of novel P-GS insertions: To identify the insertion site of each P-GS, we extracted genomic DNA from 30 frozen flies that were kept for at least 1 day at −80°. Genomic DNA was isolated following standard procedures in 150 μl Tris–HCl, 10 mm pH 7.5. Two aliquots of 5 μl of genomic DNA were digested 4 hr at 37° with the restriction enzymes *Hha*I and *Msp*I, respectively. Following heat inactivation of the enzymes by 20 min incubation at 65°, 5 μl of each digestion were incubated for 2 hr at room temperature with T4 ligase in a final volume of 200 μl. We used 5 μl of ligation in 50 μl to set inverse-PCR reactions using the 3′ P-specific oligonucleotides CTTCTTGGCAGATTTCAGTAGTTGC and ATTGCAAGCATACGTTAAGTGGA or the 5′ P-specific oligonucleotides CTTCTTGGCAGATTTCAGTAGTTGC and GTG TATACTTCGGTAAGCTTCG. The PCR parameters were: 95° for 5 min, 35 cycles of 95° (45 sec), 55° (1 min), 72° (2 min), and a 10-min extension at 72°. The PCR products were visualized in agarose 1%, purified using the Promega PCR-purification

kit, and sequenced with the oligonucleotide CGACGGGAC CACCTTATGTTA. The resulting sequences were nBlast in the NCBI database, and the adjacent genes were annotated.

EST clones: We used the following EST cDNA clones obtained from the Berkeley Drosophila Genome Project: LD22609 (*CG9056*), LD12946 (*CG9066*), LD21622 (*shi*), RH08992 (*CG15916*), LP05693 (*Stat92E*), AT20145 (*att*), AT12489 (*CG5180*), RH34302 (*CG15922*), LP04613 (*CG10877*), RE08174 (*CG11617*), and LD23468 (*yrt*) y GH14210 (*CG5191*).

Generation of constructs: To express the *yurt* (*yrt*) gene under control of the UAS promoter we used the full-length cDNA LD23468. The insert was liberated with *Eco*RI and *Eco*RV and cloned in pBluescript II SK+ (Stratagene, La Jolla, CA). Of this construct, the insert was liberated with *Not*I and *Kpn*I and cloned in pUAST (Brand and Perrimon 1993). Several *UAS-yrt* lines were established after germ-line transformation following standard procedures.

Immunocytochemistry: We used rabbit anti-phosphorylated Mad (Tanimoto *et al.* 2000) and anti-β-galactosidase (Cappel), mouse monoclonal anti-Bs, and anti-CD2 (Serotec, Oxford). Secondary antibodies were from Jackson Immunological Laboratories (used at 1/200 dilution). Pupal wings were dissected, fixed, and stained as described in de Celis (1997). Confocal images were captured using a Bio-Rad (Hercules, CA) confocal microscopy.

***In situ* hybridization:** We used digoxigenin-labeled RNA probes synthesized from the corresponding EST clones. Third instar larvae were dissected in PBS and fixed 30 min in 4% paraformaldehide, washed three times for 5 min in PBT–0.1% Tween20, and refixed 20 min in 4% paraformaldehyde + 0.1% Tween20. After several washes in PBT–0.1% Tween20, the carcasses were kept at –20° in hybridization solution (HS: 50% formamide, 5× SSC, 100 μg/ml ADN salmon sperm, 50 μg/ml heparin, 0.1% Tween20). The hybridization was carried out overnight at 55° with 2 μl of probe in 100 μl of HS (previously denaturalized by 10 min incubation at 80°). Excess of probe was washed at 55° in HS, and discs were washed several times in PBT–0.1% Tween20 and incubated for 2 hr with anti-digoxigenin antibody (Roche, Indianapolis) in a 1:4000 dilution in PBT–0.1% Tween20. The color reaction was carried out in 100 mm NaCl, 50 mm $MgCl_2$, 100 mm Tris–HCl pH 9.5, 0.1% Tween20, nitroblue tetrazolium chloride, and bromo-chloro-indolyl-phosphate (Roche). After the color developed, the discs were rinsed several times in PBT–0.1% Tween20, dissected in 30% glycerol, and mounted in 70% glycerol.

RESULTS

Effects on wing vein formation caused by modifications in the activity of signaling pathways during pupal development: The expression of target genes of the Notch, EGFR, and Dpp signaling pathways is related to the development of veins during imaginal and pupal stages. Thus, the expression of *argos*, *Star*, *MKP3*, and dP-ERK, all members of EGFR signaling, is increased in the veins during imaginal development, whereas the expression of *E(spl)m*β, a target of Notch, is higher at the boundaries between the veins and the interveins (de Celis 2003). These domains of signaling are maintained during pupal development, when the Dpp target P-Mad is also detected in the developing veins (de Celis 2003). The activity of the Notch, EGFR, and Dpp signaling pathways is required for the differentiation of veins with the correct thickness (de Celis 2003). In fact, interfering with the activity of these pathways during pupal development causes very reproducible phenotypes in the adult wing (Sotillos and De Celis 2005 and Figure 1, G–L). We have used these phenotypes as the base for a genetic screen to identify novel elements belonging to these signaling pathways, as well as other genes affecting vein formation during pupal development. To this end, we mobilized a P-GS element and looked for phenotypes affecting the wing in flies carrying newly generated P-GS insertions and a Gal4 line expressed in the developing pupal veins (*Gal4-shv^{3Kpn}*, see Figure 1, A–C). As a preliminary pilot experiment we established 180 P-GS stocks and crossed all of them with *Gal4-shv^{3Kpn}*, to estimate the viability of the resulting combinations and the frequency of mutant phenotypes. We obtained 95% viability in these combinations, with 10% of lines causing discernible phenotypes in the wing. The high viability of combinations involving *Gal4-shv^{3Kpn}* allows screening P-GS/*Gal4-shv^{3Kpn}* *trans*-heterozygotes without previously establishing balanced P-GS stocks.

Phenotypic classes and distribution of insertion sites of novel P-GS: We generated 12,853 P-GS insertions as w^+ males (5171) and females (7682) and crossed them to *Gal4- shv^{3Kpn}* flies in groups of 5 P-GS/+ individuals to 10 *Gal4-shv^{3Kpn}* siblings. Among the progeny we selected 493 P-GS insertions that, in combination with *Gal4-shv^{3Kpn}*, gave a phenotype in the wing. The insertion site of the P-GS elements was identified for 95% of the insertions by inverse PCR (see materials and methods). The 469 P-GS elements mapped to 254 insertion sites, the majority of them (149) corresponding to single hits (Figure 2A). This distribution, together with the preferential localization of P-GS elements within the 5′ end of the affected genes (Figure 2B), and the appearance of well-known hot spots, are characteristic of *P* elements (Liao *et al.* 2000). In general, independent P-GS insertions mapping in the proximity of the same gene or genes cause similar phenotypes in combination with a variety of Gal4 lines (data not shown).

The modifications to the wing pattern of P-GS/*Gal4-shv^{3Kpn}* combinations were grouped into five phenotypic classes: (1) vein thickening (V+), (2) loss of veins (V−), (3) defects in dorsal–ventral apposition (B), (4) wing folding (F), and (5) abnormal trichome differentiation (CD). The frequency of insertion sites belonging to each phenotypic class is shown in Figure 2C. The most frequent phenotype we observed, corresponding to 30% of the insertion sites, consists of the appearance of thicker than normal veins. This phenotype results from the differentiation of more than normal provein cells as vein and might be caused by failures in the lateral inhibition mechanism restricting the number of vein cells within each provein. The thickening of veins is variable and affected all veins or only individual veins (Figure 3, D–F). The veins were thickened homogeneously along their entire length (Figure 3D), or,

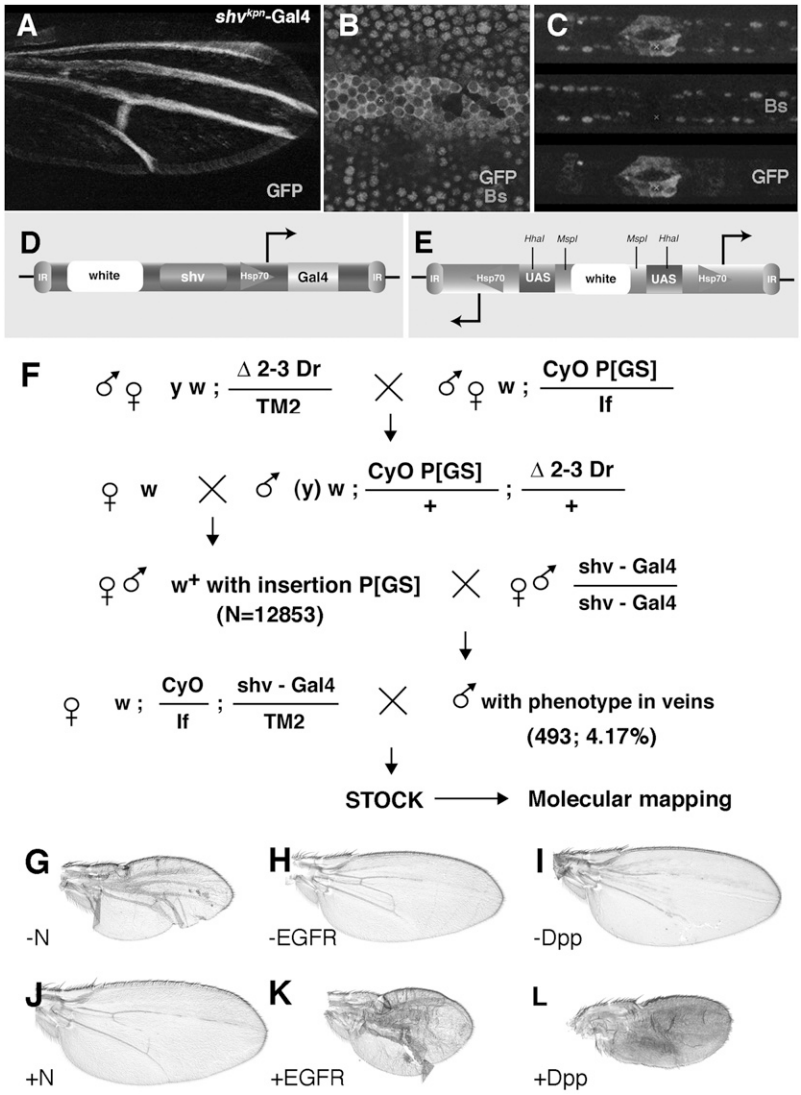

FIGURE 1.—Gal4 and P-UAS lines used in the screen, schematic of the genetic crosses, and modifications to the vein pattern resulting from modifications in the Notch, EGFR, and Dpp signaling pathways during pupal development. (A) Expression of green fluorescent protein (GFP) in *Gal4-shv^{3Kpn}/UAS-GFP* pupal wings 36 hr APF. (B) Higher magnification of the vein L3 showing expression of GFP in the cell membranes of vein cells and expression of Blistered (Bs) in the nucleus of intervein cells. (C) Tangential section of B showing the complementary domains of Bs and GFP expression in the intervein and vein, respectively. (D) Representation of the *Gal4-shv^{kpn}* vector. (E) Representation of the P-GS vector showing the UAS sequences and *Hsp70b* promoter near the inverted terminal repeats (IR) at both *P*-element ends. The *mini-white* gene (white) and the position of the restriction sites used to map the P-GS insertions (*Hha*I and *Msp*I) are indicated in E. (F) Generation of new P-GS insertions using Δ2-3 transposase to mobilize a P-GS element inserted on a CyO chromosome. The flies with a novel P-GS insertion were crossed to *Gal4-shv^{3kpn}* flies to induce the expression of the genes adjacent to the vector, and flies with a wing mutant phenotype were selected to establish balanced lines. (G) Ectopic expression in the pupal veins of a dominant-negative form of Notch (*Gal4-shv^{3Kpn}/UAS-N^{ecd}*; −N) results in strong thickening of the veins. (H) Ectopic expression of a dominant-negative form of EGFR (*Gal4-shv^{3Kpn}/UAS-EGFR^{DN}*; −EGFR) causes loss of veins. (I) Expression of the Dpp-antagonist Dad (*Gal4-shv^{3Kpn}/UAS-dad*; −Dpp) causes loss of veins. (J) Expression of the intracellular fragment of Notch (*Gal4- shv^{3Kpn}/UAS-N^{intra}*; +N) eliminates the veins. (K) Expression of an activated form of the EGFR downstream component Ras (*Gal4- shv^{3Kpn}/UAS-Ras^{V12}*; +EGFR) causes the formation of thicker veins. (L) Expression of the ligand Dpp (*Gal4-shv^{3Kpn}/UAS-dpp*; +Dpp) causes the differentiation of most wing tissue as vein.

alternatively, they differentiated stretches of vein tissue irregularly thickened (Figure 3E). The second phenotype affecting exclusively the veins consists of the loss of vein tissue and is characteristic of 16% of insertion sites (Figure 3, A–C). Individual P-GS insertions combined with *Gal4-shv^{3Kpn}* display different intensities of vein loss, affecting either individual veins (generally L4, Figure 3C) or the distal ends of all longitudinal veins (Figure 3, A and B). Because the *Gal4-shv^{3Kpn}* driver is expressed only during pupal development, loss of veins must result from the failure to differentiate as vein of provein cells that were previously specified as such in the corresponding imaginal disc. The third and fourth phenotypic classes, loss of dorsal–ventral apposition and wing folding, include 20 and 12% of the insertion sites, respectively (Figure 2C). In many instances, these two phenotypes appeared simultaneously in the same wing; *i.e.*, the wing is folded and the dorsal–ventral apposition fails (Figure 3, G and H). The apposition between the dorsal and ventral surfaces is a complex process that takes place during pupal development, after the eversion of the wing disc. In this process, the dorsal and ventral wing surfaces become adhered through their basal cell membranes, and several molecules involved in adhesion between cells or between cells and the extracellular matrix play a preeminent role (BLOOR and BROWN 1998; WALSH and BROWN 1998). Wing folding and dorsal–ventral defects are also observed upon interferences with the programmed cell death that wing cells undergo during metamorphosis and eclosion (KIGER *et al.* 2001; KIMURA *et al.* 2004). Thus, genes included in these categories might affect a variety of processes including cell viability, extracellular matrix formation, or cell adhesion.

In addition to vein differentiation and wing morphogenesis, we also identified a number of insertion sites (22%) that result in cell differentiation defects in combination with *Gal4-shv^{3Kpn}* (Figure 2C). These phenotypes

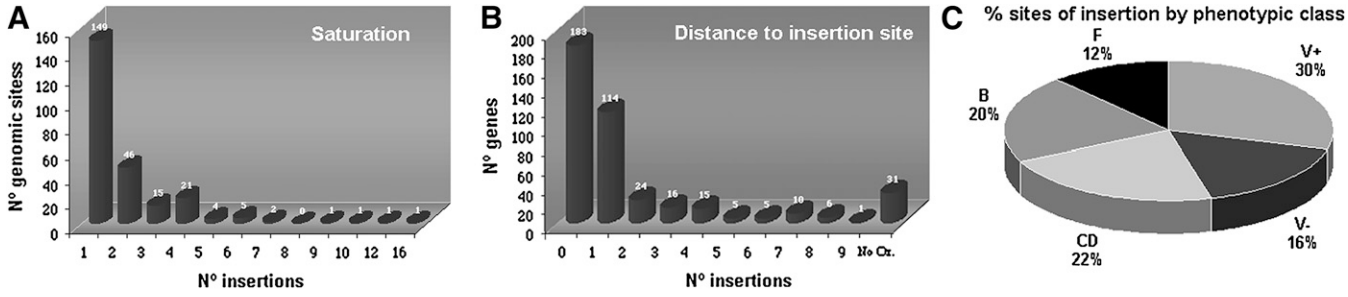

FIGURE 2.—Numerical parameters of the screen. (A) Genomic sites identified grouped by the number of P-GS insertions located in a similar position (±1 kb) in the molecular map. Most genomic sites have been identified by only one insertion (149). (B) Distance of P-GS insertions to the closest adjacent gene. Most of the insertions are situated within a gene or at a distance of <1 kb (183). (C) Frequency of phenotypic classes in the combinations between P-GS insertions and *Gal4-shv*^{3kpm}: 30% of insertion sites result in thicker veins (V+), 16% produce loss of veins (V−), 22% cause alterations in trichome differentiation (CD), 20% cause defects in dorsal–ventral apposition (B) and 12% result in misfolded wings (F).

include loss or incorrect formation of hairs (Figure 3, I and J), differentiation of several hairs per cell, and the formation of hairs of smaller than normal size (Figure 3, K–M). Hair morphogenesis relies on the correct polymerization of actin in the distal-most apical region of wing cells (prehair), in a process dependent on the establishment of correct planar cell polarity (ADLER 2002). Therefore, genes modifying hair morphogenesis and number might be affecting actin dynamics and/or planar cell polarity.

Ectopic gene expression associated with P-GS insertions: The P-GS vector carries UAS sequences at both its 5′ and its 3′ends and may affect genes located at both sites of the insertion site (TOBA *et al.* 1999). The advantage of this disposition of flanking UAS sequences is that several genes are targeted at the same time by unique P-GS insertions, increasing the frequency of phenotypes associated with P-GS in comparison with other EP elements (TOBA *et al.* 1999). However, the simultaneous overexpression of more than one gene by each P-GS greatly complicates the identification of the gene responsible for the mutant phenotype. To assess the range of P-GS effects on adjacent genes, we carried out *in situ* hybridization with RNA-labeled probes of genes adjacent to several P-GS insertions. We found that in all the cases analyzed (21, data not shown) the genes

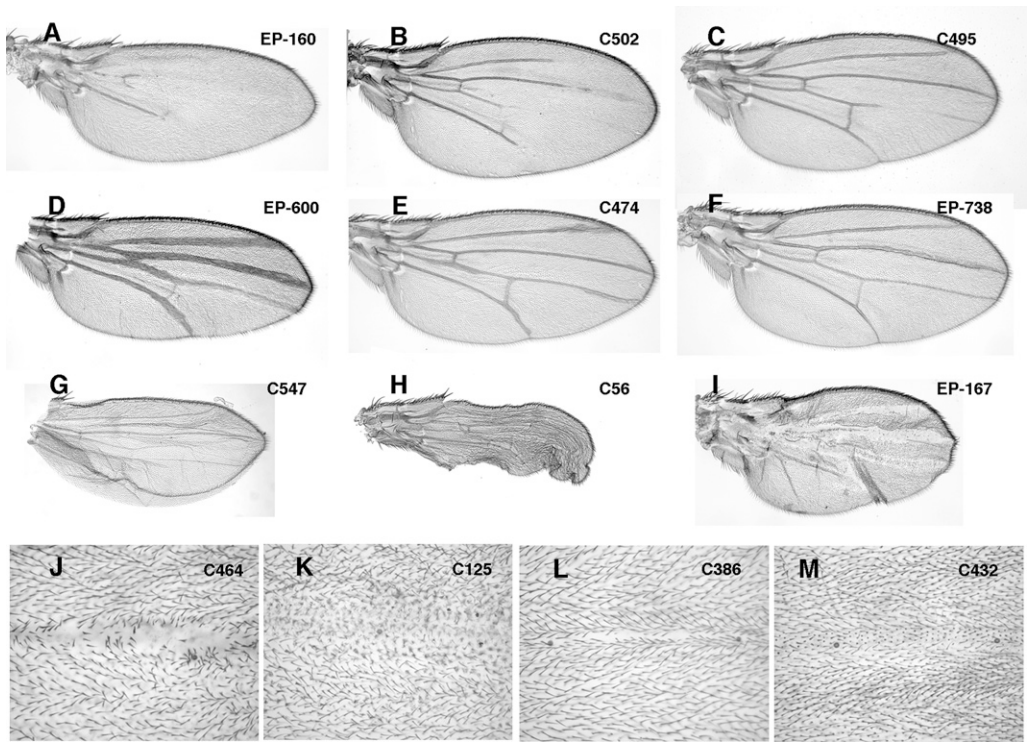

FIGURE 3.—Representative phenotypes obtained in the combinations of P-GS lines with *Gal4-shv*^{3kpm}. (A–C) Loss of vein differentiation: strong phenotype (A, *Gal4-shv*^{3kpm}/EP-160), weak phenotype (B, *Gal4-shv*^{3kpm}/C502) and loss of the L4 vein (C, *Gal4-shv*^{3kpm}/C495). (D–F) Vein thickening: strong phenotype (D, *Gal4-shv*^{3kpm}/EP-600), weak phenotype (E, *Gal4-shv*^{3kpm}/C474) and thickened L3 vein (F, *Gal4-shv*^{3kpm}/EP-738). (G) "Blistered" or dorsal–ventral apposition phenotype (*Gal4-shv*^{3kpm}/C547). (H) Folded wing (*Gal4-shv*^{3kpm}/C56). (I) Vein thickening and loss of trichome differentiation phenotype (*Gal4-shv*^{3kpm}/EP-167). (J–M) Higher magnification of the L3 vein showing cell differentiation defects such as loss of trichomes (J, *Gal4-shv*^{3kpm}/C464), differentiation of several trichomes per cell (K, *Gal4-shv*^{3kpm}/C125), loss of trichomes and reduced pigmentation (L, *Gal4-shv*/C386), and formation of smaller than normal trichomes (M, *Gal4-shv*^{3kpm}/C432).

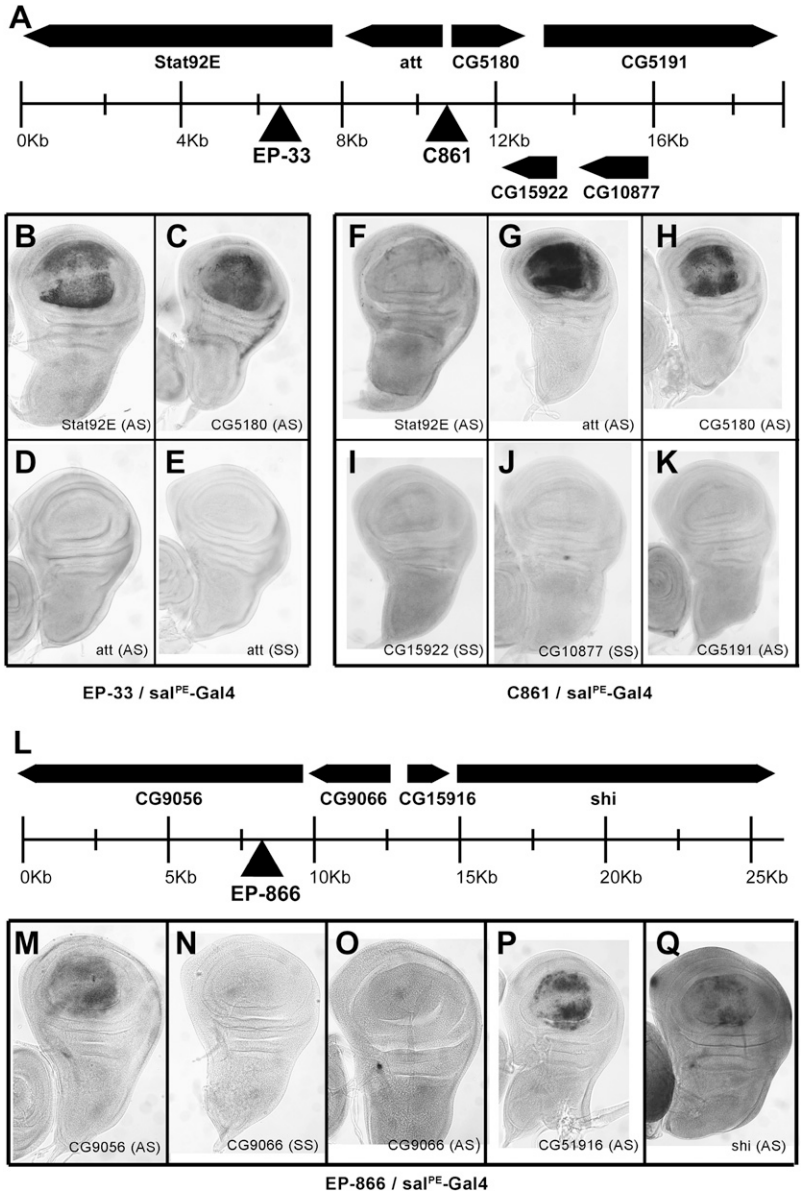

FIGURE 4.—Effects of P-GS insertion on adjacent genes. (A) Schematic of the genomic region where the P-GS insertions *EP-33* and *C861* (triangles) are localized, showing the annotated transcription units as horizontal thick solid arrows. (B–E) *In situ* hybridization with *Stat92E* (B), *CG5180* (C), and *att* (D) antisense probes and with *att* sense probe (E) in *EP-33/Gal4-sal* wing imaginal discs. Ectopic expression in the *spalt* domain is detected only for *Stat92E* (B) and *CG5180* (C) and no expression is detected for the transcript oriented "antisense" with respect to the insertion site (*att* in D). (F–K) *In situ* hybridization with *Stat92E* (F), *att* (G), *CG5180* (H), and *CG5191* (K) antisense probes and with sense probes for the transcripts *CG15922* (I) and *CG10877* (J) in *C861/Gal4-sal* wing imaginal discs. Ectopic expression is only detected for the transcripts *att* (G) and *CG5180* (H) and no Gal4-driven expression is detected for the transcript with antisense orientation (*CG15922* in I and *CG10877* in J). (L) Schematic of the genomic region where the P-GS insertion *EP-866* (triangle) is localized. (M–Q) *In situ* hybridization with *CG9056* (M), *CG9066* (O), *CG15916* (P), and *shi* (Q) antisense probes and with *CG9066* sense probe (N) in *EP-866/Gal4-sal* wing imaginal discs. Ectopic expression is detected for the three transcripts oriented "sense" with respect the insertion site (*CG9056*, *CG15916*, and *shi*), whereas no expression is detected for the transcript with antisense orientation (*CG9066*).

located at both ends of a given P-GS insertion are expressed under UAS control when they are in the outward transcriptional orientation with respect to the insertion site (data not shown). In addition, in none of four cases analyzed did we observe transcription of antisense RNA, suggesting that most of the observed phenotypes correspond to the ectopic expression of sense RNAs and not to RNA interference caused by ectopic antisense expression. We further analyzed the range of P-GS effects by *in situ* hybridization in two clusters of six and four genes, respectively, placed in different orientations and spanning ~30 kb of genomic DNA. In the first case the insertion sites of EP-33 and C861 are separated by 8 kb of DNA and the genes *Stat92E*, *att*, *CG5180*, *CG15922*, *CG10877*, and *CG5191* map in their vicinity (Figure 4A). In the second case, the EP-866 insertion maps in the vicinity of the transcription units *CG9056*, *CG9066*, *CG15916*, and *shi* (Figure 4L). In both cases no transcription is detected using sense probes for transcripts oriented toward the insertion site (*att* for EP-33, *CG15922* and *CG10877* for C861, and *CG9066* for EP-866; Figure 4, E, I, J, and N, respectively). Similarly, the genes *att* and *CG9066* are not ectopically transcribed in *EP-33/Gal4-sal* and *EP-866/Gal4-sal* discs, respectively, despite being adjacent to the EP-33 and EP-866 insertions (Figure 4, D and O). We find that two adjacent genes in the forward orientation can be simultaneously overexpressed (*CG15916* and *shi* in EP-866, Figure 4, P and Q), even though they are separated from the insertion site by a transcription unit (*CG9066*, Figure 4, N and O) in the antisense orientation (Figure 4, L, N, and O). In this case the efficiency of transcription appears to be higher for the gene localized closer to the insertion site (compare Figure 4P with 4Q).

However, in other pairs of genes in the forward orientation to the C861 insertion, *CG5180/CG5191* and *Stat92E/att*, we could detect expression only of the genes localized closer to the insertion site (Figure 4, F–H and K). These observations suggest that the range and efficiency of P-GS insertions to drive expression of neighboring genes depend on the genomic environments. With our data we cannot determine the maximal distance of a P-GS insertion to a gene compatible with gene expression regulated by UAS sequences. It is clear, however, that the adjacent genes located within 0–10 kb of the insertion site in a "forward" orientation are the best candidates to be affected by UAS sequences and therefore responsible for the gain-of-expression phenotype. The complete list of mapped P-GS insertions and the candidate genes associated with each of them are shown in Table 1.

Comparison between P-GS insertion and UAS constructs: To assign the gene responsible for the ectopic-expression phenotype in several insertions, we compared the phenotypes resulting from combining a Gal4 driver with either the P-GS or the UAS lines of the candidate gene/s. In all cases analyzed (26) the phenotype observed in the Gal4/P-GS combination was very similar to that resulting from the UAS/Gal4 combination (Table 2, Figure 5, and data not shown). In six P-GS insertions (C279, EP-36, EP-E, EP-459, C107, and C192; Table 2) there was only one gene located in the forward orientation in the proximity of the P-GS insertion (Table 2). In all these cases the phenotypes of the combinations involving the P-GS and the corresponding UAS line were very similar (Figure 5, A and E, B and F, and D and H). In 3 cases (C166, C865, and EP-23) there were two candidate genes for each insertion. The phenotype of these P-GS/Gal4 combinations could be ascribed, however, to only one of the two ectopically expressed genes (Figure 5 and Table 2). In 4 cases the P-GS insertions are flanked by one gene located in the forward orientation and the other gene in the "backward" orientation. In these cases the analysis of phenotypes caused by UAS/Gal4 combinations allowed us to ascribe the phenotype of P-GS/Gal4 combinations to the gene located in the forward orientation (Figure 5, C and G). Finally, in 7 cases where two candidate genes were oriented in the forward orientation with respect to the P-GS insertion we were able to identify the gene responsible for the overexpression phenotype either by using UAS-RNAi of the candidate genes or by mapping chemically induced reversions (data not shown). In the first case, the expression of one UAS-RNAi was able to suppress the mutant phenotype of the P-GS/Gal4 combination, and, in the second case, chemically induced revertants of the P-GS/Gal4 combination mapped to the coding region of one of the candidate genes (see Ruiz-Gomez *et al.* 2005). These data suggest that, for most P-GS insertions, it is likely that the phenotype is caused by only one of the several genes being ectopically expressed. However, in the annotation of candidate genes, we took the parsimonious criterion that all genes located within 10 kb distance to the insertion site and placed in the forward orientation to this site were candidates to mediate the phenotypes of P-GS/Gal4 combinations (see below).

Phenotypic specificity of novel P-GS insertions: Most known genes affecting vein differentiation are also required in other developmental processes. Thus, it is expected that the genes we identified affecting vein patterning or wing morphogenesis when overexpressed during pupal development will also affect other tissues in combinations between the P-GS insertions and other tissue-specific Gal4 lines. This is the case when any UAS line of known elements of the Notch, EGFR, and Dpp signaling pathways is combined with a variety of Gal4 drivers expressed at different developmental times and tissues (data not shown). To evaluate whether the new P-GS insertions are able to modify other developmental processes in addition to wing vein formation, we made combinations between all P-GS insertions and Gal4 lines expressed in proneural clusters (*Gal4-253*) and in the wing blade during imaginal development (*Gal4-638*). Forty-five percent of *P-GS/Gal4-253* combinations display mutant phenotypes affecting the macro- and/or microchaeta in the fly thorax and abdomen (Table 3, Figure 6). These phenotypes were of different expressivity and include loss of chaetae, apparition of extra-chaetae, and differentiation of chaetae with abnormal size and/or shape (Table 3, Figure 6). The extra-macrochaetae appear usually close to the normal macrochaetae, either forming clusters of adjacent macrochaetae or in groups of several macrochaetae separated by intervening trichomes, suggesting failures in lateral inhibition (Figure 6, D, F, and H). About 83% of P-GS insertions cause wing phenotypes in combination with the wing-specific driver *Gal4-638* (Table 3). These phenotypes include pupal lethality, loss of wing tissue accompanied by vein pattern alterations (Figure 6C), different degrees of wing margin loss (Figure 6, A, C, E, and G), blistered and misfolded wings, loss of veins, and differentiation of thicker or ectopic vein tissue (Figure 6, E, G, I, and K). We also combined 70 selected P-GS lines with the Gal4 drivers *Gal4-dll* and *Gal4-ey*, expressed in the leg and eye imaginal discs, respectively. We obtained a mutant phenotype in 86% (*Gal4-dll*, data not shown) and 57% (*Gal4-ey*, data not shown) of these combinations. Taken together, these data indicate that there is no specificity of tissue or developmental time for most genes selected by their ectopic expression phenotypes in the pupal wing. However, we could find several correlations when comparing the phenotypes caused by P-GS insertions in combination with different Gal4 lines that might be indicative of specificity in the developmental mechanisms affected (Figure 7). For example, most P-GS lines affecting the veins during pupal development also affect the veins in a similar manner

TABLE 1

Insertion sites and candidate genes identified in the screen

P-GS line (no. insertions)	Citology	*shv*-Gal4	*D*	5′ gene	Molecular class	No. candidates	*D*	3′ gene	Molecular class
C649 (1)	1E3	B				0			
EP-63 (1)	3A1	V−	3	*CG14049 (Ilp6)*	CS	2	7	*CG2845 (phl)*	CS
EP-489 (1)	3C6	V+				1	1	*CG3653 (kirre)*	CS, CA
EP-A (2)	3C7	V+				1	0	*CG3936 (N)*	CS
C155 (3)	4B2	V+	1	*CG3665 (Fas2)*	CA	1			
EP-B5 (1)	4C4	F				1	0	*CG3578 (omb)*	TF
EP-620 (4)	4E2	CD	0	*CG32767*	TF	1			
EP-469.2 (4)	5B5	V−	1	*CG3171 (Tre1)*	CS	2	1	*CG15779 (Tre)*	CS
C684 (1)	7C4	B	0	*CG10778*	M	2	1	*CG1524 (RpS14a)*	RB
C858 (1)	8B4	V+	0	*CG10701 (Moe)*	CY	1			
C76 (1)	9D2	V+	2	*CG15302 (or9a)*	CS	2	0	*CG15304*	CG
EP-165 (6)	9E1	V+	1	*CG32676*	PP	2	0	*CG1799 (ras)*	M
C719.2 (1)	9F5	CD	1	*CG1655*	CS	2	0	*CG2186*	CG
EP-1052 (1)	9F5	Dif	0	*CG11207 (feo)*	CY	2	4	*CG2186*	CG
EP-Z (1)	10C9	V+	0	*CG1697 (rho-4)*	CS	1			
EP-694 (1)	11A11	Pol	1	*CG1900 (Rab40)*	CS	2	1	*CG17788*	CG
EP-332 (1)	11D1	F	6	*CG33651*	CG	1	NO		
EP-689 (1)	12E5	CD	NO			1	0	*CG12047 (mud)*	CGh
EP-457 (5)	12F4	B	0	*CG9533 (rut)*	M	2	7	*CG14411*	M
C373 (3)	13F1	B	NO			1	1	*CG8544 (sd)*	TF
C736 (2)	13F17	V−	0	*CG9056*	CG	1			
C375 (1)	15C4	CD	1	*CG9089 (wus)*	PP	1	NO		
EP-493 (1)	15F4	B	3	*CG8915 (helicasa)*	RB	2	2	*CG12996*	CG
C832 (1)	16C1	B	0	*CG32556*	CG	1			
EP-631 (1)	16C1	CD	1	*CG32556*	CG	2	4	*CG5884 (par-6)*	CA
C800 (1)	17A8	B				1	0	*CG6103 (CrebB-17A)*	TF
EP-471 (1)	21B2	V+	NO			1	0	*CG18497 (spen)*	TF
EP-234 (1)	21B4	V−	2	*CG11617*	TF	1			
C31 (1)	21C2	V+	0	*CG11907 (Ent1)*	M	1			
C580 (1)	21C4	wt	NO			1	0	*CG4114 (ex)*	CS
EP-67 (2)	21C6	Pol				0			
C480 (4)	21C6	CD	0	*CG4427 (cabut)*	TF	1			
EP-822 (1)	21D1	V+	1	*CG17941 (ds)*	CS, CA	1			
EP-720 (2)	22C1	V+	2	*CG15378 (lectin-22C)*	M	2	0	*CG4244 (su(dx))*	PP
C676 (2)	22E1	V+	0	*CG3664 (Rab5)*	CS	2	0	*CG4272*	CS, CD
C517 (3)	22F2	V+				1	6	*CG9885 (dpp)*	CS
EP-500.2 (1)	24A1	B	0	*CG10033 (for)*	CS	1			
C37 (2)	24C3	B	NO			1	0	*CG10021 (bowl)*	TF
C544 (1)	25B1	B	NO			1	1	*CG3036*	M
EP-322	25B10	F	0	*CG33113 (Rtnl1)*	CS	1			
EP-800 (1)	25B3	F	0	*CG8890 (Gmd)*	CS	1			

(*continued*)

TABLE 1

(Continued)

P-GS line (no. insertions)	Citology	*shv*-Gal4	*D*	5′ gene	Molecular class	No. candidates	*D*	3′ gene	Molecular class
C575 (1)	25B9	F	1	*CG8892*	PP	2	7	*CG31653*	CG
EP-787 (1)	25C1	B	8	*CG8680*	M	1			
EP-472 (1)	26A1	Dif	2	*CG9021*	CG	2	0	*CG14001 (bchs)*	PP
C174 (3)	26A5	CD	0	*CG9553 (chic)*	CY	2	2	*CG9075 (eIF-4a)*	RB
C386 (2)	26B2	CD	0	*CG9088 (lid)*	TF	2	1	*CG9093 (Tsp26A)*	CS
C446 (4)	26B3	F	1	*CG9154*	CGh	2	0	*CG9159 (Kr-h2)*	TF
EP-603 (2)	27F1	Dif	NO			1	3	*CG5261*	M
EP-M71 (1)	27F3	CD				1	0	*CG4971 (Wnt10)*	CS
EP-600	28D1	V+				1	0	*CG7123 (LanB1)*	CA
EP-899 (2)	28D3	V−	1	*CG7233 (snoN)*	CS, TF	1			
EP-24 (4)	29A1	V+	0	*CG8049 (Btk29A)*	CS	1			
EP-232 (1)	29C3	V+	1	*CG13398*	CS	2	1	*CG13388 (Akap200)*	CS
C503 (3)	29C3	F	4	*CG13398*	CS	2	0	*CG13388 (Akap200)*	CS
C717 (2)	30B5	V+, CD	0	*CG4405 (jp)*	CY	2	2	*CG3838*	Cgd
C388 (4)	30B8	CD	1	*CG4422 (Gdi)*	CS	1			
C282 (1)	30C7	B				1	0	*CG3998 (zf30c)*	TF
EP-108 (1)	30F4	V+	1	*CG5838 (Dref)*	TF	2	0	*CG4651 (RpL13)*	RB
C488 (1)	30F5	V+				1	1	*CG4722 (bib)*	CS
EP-112 (2)	31A1	V−	NO			1	0	*CG4799 (Pen)*	M
EP-731 (1)	31E1	Dif	0	*CG5355*	PP	2	1	*CG5300 (Klp31E)*	CY
C242 (1)	32B1	F	0	*CG6647 (porin)*	M	2	1	*CG17085*	CG
EP-179 (1)	32E1	B	0	*CG4807 (ab)*	TF	1			
EP-(19) (1)	32E2	V−	1	*CG6392 (cmet)*	CY	2	0	*CG32955 (Cana)*	CY
EP-476 (1)	32F2	Dif	0	*CG31705*	CG	1	NO		
EP-Ib (6)	33A1	B	0	*CG14938 (crol)*	TF	1	NO		
EP-M32 (2)	33B3	V+	1	*CR31863 (bft)*	snRNA	1			
C762 (2)	33F4	V−	1	*CG12283 (kek-1)*	CS	1			
EP-1008 (2)	34D4	V+				1	1	*CG7793 (Sos)*	CS
C891 (2)	35A3	B	1	*CG4551 (smi35A)*	CS	1			
C143 (16)	35D2	CD	0	*CG3758 (esg)*	TF	1			
EP-339 (5)	35E2	V−	0	*CG4993 (PrL-1)*	CS	2	7	*CG4930*	CG
C17 (5)	35F1	V−	0	*CG7664 (crp)*	TF	2	1	*CG4132 (pkaap)*	CS
EP-64 (1)	36A2	B	1	*CG5953*	CG	1			
C877 (1)	36A2	V+	8	*CG4952 (dac)*	TF	2	0	*CG4599 (Trp2)*	PP
EP-M (2)	36C5	V+	0	*CG6667 (dl)*	TF	2	3	*CG5050*	CG
EP-323 (2)	37B11	V−	1	*CG15173*	CGd	2	0	*CG10473*	CD
C623 (1)	37D7	CD	0	*CG10334 (spi)*	CS	1			
C719.1 (1)	38E3	B	1	*CG9318*	M	2	0	*CG2637 (Fs(2)Ket)*	M
C359 (1)	38F1	B	NO			1	0	*CCG31673*	M
C277 (6)	39B4	V+, CD	1	*CG31626*	CG	2	0	*CG8676 (Hr39)*	TF
EP-319 (2)	42A4	CD	0	*CG12051 (Act42A)*	CY	2	0	*CG7865 (PNGase)*	PP

(*continued*)

TABLE 1

(Continued)

P-GS line (no. insertions)	Citology	*shv*-Gal4	*D*	5′ gene	Molecular class	No. candidates	*D*	3′ gene	Molecular class
C504 (2)	42E1	F	1/4	*CG3572 (vimar)/CG30156*	CS/PP	3	0	*CG17002*	CG
C109 (1)	42E4	F	7	*CG3572 (vimar)*	CS	3	0/0	*CG18742 (Tsp42Ea)/CG30159*	CS
C573 (1)	42E5	F	1	*CG12846 (Tsp42Ed)*	CS	2	0	*CG10106 (Tsp42Ee)*	CS
C371 (2)	43B1	B	1	*CG1708 (cos)*	CY	2	1	*CG11107*	RB
EP-3 (3)	44C2	V−	1	*CG3161 (dpn)*	TF	1			
C434.2 (1)	44C4	V+, CD	NO			0			
EP-405 (1)	44E3	CD	0	*CG8739 (cmp44E)*	CA	2	3	*CG8740*	CG
C935 (1)	44F7	CD	0	*CG8248*	CY	2	1	*CG8243*	CS
EP-M89 (1)	45C3	V−	1	*CG2072 (TXBP181-like)*	CGh	2	0	*CG1975 (Rep2)*	CGd
EP-65 (1)	45F1	V−	7	*CG1888*	CG	2	1	*CR33010 (mir-14)*	microRNA
EP-23 (6)	46C4	V−	0	*CG1429 (Mef2)*	TF	1			
C356 (1)	46D7	V+	1	*CG18445*	CGh	2	0	*CG2249*	M
EP-878	47A1	B	0	*CG3298 (JHI-1)*	RB	2	0	*CG12909*	RB
C839 (1)	47C1	CD	1	*CG12342*	CGd	2	0	*CG12323 (Pros b5)*	PP
C192 (4)	47D7	B	0	*CG7734 (shn)*	CS, TF	1			
C170 (3)	48A2	F	0	*CG10897 (tou)*	TF	1	NO		
C7 (1)	49A4	V+, CD	4	*CG8834*	M	2	0	*CG8525*	M
C478 (1)	50C14	V+	0	*CG6671 (AGO1)*	RB	3	0/0	*CG33155/CG30481 (mRpL53)*	CG/M
EP-990 (3)	50D1	V+				1	0	*CG8118 (mam)*	CS
C56 (4)	50E6	F	1	*CG8542 (Hsc70-5)*	M	2	0	*CG8531*	M
EP-608 (2)	51E3	F				1	0	*CG11798 (chn)*	TF
C603 (1)	51F11	CD	1	*CG8171 (dup)*	TF	2	0	*CG8174 (SRPK)*	CS
C207 (1)	52A8	F	0	*CG8183 (Khc-73)*	CY	2	5	*CG30471*	CG
EP-M21 (1)	52D9	wt	0	*CG8322 (ATPCL)*	M	2	2	*CG8370*	CGh
C27 (2)	52F8	B	1	*CG8448 (mrj)*	M	1	NO		
C231 (5)	53D12	wt	NO			1	3	*CR33562 (mir8S)*	microRNA
C79 (1)	53F1	CD	NO			1	0	*CG9635 (RhoGEF2)*	CS
C459 (12)	53F9	V+	1	*CG8938 (GstS1)*	M	2	6	*CG30456*	Cgh
EP-887 (1)	54B16	wt	0	*CG6522*	CY	2	1	*CG4816 (qkr54B)*	RB, CD
EP-687 (1)	54F1	CD	3	*olf186-M*	PP	2	0	*CG11430 (olf186-F)*	PP
C367 (4)	55B7	CD	4	*CG5753 (stau)*	RB	2	0	*CG12767 (Dip3)*	TF
EP-J59 (1)	55B8	Dif	7	*CG5748 (Hsf)*	TF	2	0	*CG5119 (pAbp)*	RB
EP-773 (1)	55F6	V+, CD	1	*CG15098*	CG	2	0	*CG15083*	CG
C677 (1)	56A1	B				1	0	*CG12758 (sano)*	CG
C639.1 (2)	56C1	V+, CD	NO			1	1	*CG7097*	CS
C518 (4)	56E3	V−, CD	2	*CG9854 (hrg)*	RB	2	2	*CG11025 (IsoT-3)*	PP
EP-614 (3)	56F16	B	4	*CG13868*	CG	2	0	*CG8920*	RB
EP-709 (1)	56F8	V+				1	1	*CG8896 (18w)*	CS
C389 (2)	57A7	CD	0	*CR33617 (mir-313)*	microRNA	2	4	*CG13425 (bl)*	RB
EP-947 (1)	57C4	Dif	0	*CG30389*	CG	1			
C596 (1)	57E5	B	0	*CG10497 (Sdc)*	CS	2	7	*CG15667 (sara)*	CS

(*continued*)

TABLE 1

(Continued)

P-GS line (no. insertions)	Citology	*shv*-Gal4	*D*	5′ gene	Molecular class	No. candidates	*D*	3′ gene	Molecular class
C327.2 (1)	57E5	V+	0	*CG9847 (Fkbp13)*	PP	2	5	*CG15669 (Mesk2)*	CGd
EP-634.2 (1)	57E8	CD	8	*CG10496*	CG	2	0	*CG15669 (Mesk2)*	CGd
EP-439 (1)	57F10	V−	1	*CG30404*	CGh	2	1	*CG17952*	CA
EP-296 (1)	58D3	wt	7	*CG3413 (wdp)*	CA	2	1	*CG5820 (Gp150)*	CS
EP-575 (1)	58E4	V+	0	*CG4444 (px)*	TF	1			
EP-596 (1)	58F4	Dif	2	*CG30217*	CG	2	3	*CG4250*	CG
EP-1152.2	59B6	V−, E	1	*CG3820 (Nup214)*	M	1			
EP-O (1)	59F6	wt				1	0	*CG5393 (apt)*	TF
C125 (1)	60C7	CD	1	*CG4527 (Plkk1)*	CS	2	1	*CG3416 (Mov34)*	PP
EP-708 (1)	60D9	V−	0	*CG13594*	CG	2	1	*CG3616 (Cyp9c1)*	M
EP-261 (1)	60E1	wt	0	*CG16912*	RB	2	1	*CG3589*	PP
EP-284 (1)	60E1	V+	1	*CG16932 (Eps15)*	M	2	5	*CG3594 (Eap)*	RB
EP-644 (2)	60E5	V+				1	0	*CG9071 (NaCP60E)*	M
EP-945 (1)	61B3	wt	1	*CG17135 (E(bx))*	TF	2	1	*CG32476 (mthl14)*	CG
C293 (1)	61B3	CD	1	*CG7008 (Tudor-SN)*	TF	2	1	*CG13880 (mRpL17)*	RB
EP-880 (2)	61C3	V+	1	*CG13892 (Cypl)*	PP	2	2	*CG17090*	CS
EP-429 (1)	61F6	B	2	*CG2211*	CG	2	0	*CG9165*	M
C865 (4)	61F7	V+	0	*CG9181 (Ptp61F)*	CS	2	4	*CG1214 (ru)*	CS
C767 (1)	62A1	V+	1	*CG13916*	TF	1			
EP-450 (1)	62A3	CD	0	*CG12086 (cue)*	M	2	0	*CG1009 (Psa)*	PP
C500 (9)	63C1	V−	5	*CG12078*	CGh	2	2	*CR33598 (mir-282)*	microRNA
EP-329 (1)	64A7	B	0	*CG14995*	CD	2	1	*CG14991*	CA
C549 (1)	64D1	F				0			
C275 (2)	64E5	CD	1	*CG10578 (DnaJ-1)*	PP	2	0	*CG5486 (Ubp64E)*	PP
EP-1 (1)	65C3	V+	0	*CG10107*	PP	2	6	*CG8549*	CGh
C38 (1)	66A13	F	0	*CG17888 (Pdp1)*	TF	1			
C255 (1)	66B3	CD	6/4	*CG7574 (bip1)/CR32358*	CG/tRNA	3	8	*CG13681*	CG
C545 (1)	66C11	Dif	0	*CG7163 (mkg-p)*	TF	2	1	*CG13667*	M
C107 (3)	66D9	V−				1	0	*CG6494 (hairy)*	TF
C403 (1)	67B5	B	0	*CG3445 (phol)*	TF	2	3	*CG3552*	CG
C432 (1)	67C4	CD	1	*CG6757 (SH3PX1)*	PP	2	0	*CG16707 (vsg)*	CGd
C708 (1)	67C7	V+	3	*CG6767*	M	2	0	*CG8284 (UbcD4)*	PP
EP-730 (2)	67C9	V+	0	*CG6721 (Gap1)*	CS	1	NO		
EP-380 (1)	67D2	Pol	1	*CG6674*	CG	2	0	*CG11989 (Ard1)*	PP
C67 (1)	67F4	B	0	*CG12296 (klu)*	TF	1			
C756 (1)	68B1	B	0	*CG6190*	PP	2	1	*CG7600*	CGh
EP-297.2 (1)	68F1	V+	1	*CG12277 (rols)*	CS	1	NO		
C909 (1)	69A4	V+	0	*CG4300*	M	2	1	*CG10426*	M
EP-154 (1)	69D3	wt	0	*CG10601 (mirr)*	TF	1			
EP-872 (1)	69F4	F	NO			1	0	*CG11278 (Syntaxin13)*	PP
EP-J17b	70B1	B	0	*CG10133*	M	1	NO		

(*continued*)

TABLE 1

(Continued)

P-GS line (no. insertions)	Citology	*shv*-Gal4	*D*	5′ gene	Molecular class	No. candidates	*D*	3′ gene	Molecular class
EP-853 (1)	70B2	wt	1	*CG10083*	CY	2	1	*CG10741*	CG
EP-1013 (1)	70E5	V−	1	*CG4879 (RecQ5)*	TF	2	0	*CG5031 (dlp)*	CS
EP-501 (1)	72D6	V−	2	*CG5215 (Zn72D)*	RB	2	0	*CG5444 (Taf4)*	TF
C747 (1)	72F1	V−	0	*CG4531 (argos)*	CS	1	NO		
C427 (1)	73D1	V+, CD	3	*CG9668 (Rh4)*	CS	2	0	*CG11914 (Lmpt)*	TF
EP-666 (1)	73D1	F				1	0	*CG9712 (TSG101)*	PP
C153 (2)	74D2	F	4	*CG6311*	CGh	2	0	*CG7555 (Nedd4)*	PP
EP-182 (1)	75B1	B				1	0	*CG8127 (Eip7B)*	TF
C272 (1)	75D1	B	1	*CG13702 (AlCR2)*	CS	1			
EP-160 (3)	75F6	V−	1	*CG14080 (Mkp3)*	CS	1			
EP-P (2)	76D1	B	0	*CG8742 (Gyc76C)*	CS	2	3	*CG8522 (HlH106)*	TF
C752 (1)	76D3	B	0/1	*CG8103 (Mi-2)/CG32217*	PP	3	0	*CG7757*	RB
C474.1 (2)	77B4	V+	1	*CG5585*	CGh	2	0	*CG5605 (eRF1)*	RB
C167 (1)	78B1	B	4	*CG10564 (Ac78C)*	CS	2	0	*CG32435 (chb)*	CY
EP-17 (3)	83A5	V−	0	*CG2899 (ksr)*	CS	2	2	*CG31550*	TF
EP-256 (4)	85C1	V−	1	*CG11988 (neur)*	CS	1			
C606 (2)	85C4	CD	0	*CG9755 (Pum)*	RB	1			
C926 (1)	85D1	V−	2	*CG9746*	CS	1			
C343 (1)	85D21	V+	1	*CG9375 (Ras85D)*	CS	2	0	*CG8161 (Rlb1)*	CGd
EP-643 (2)	85D22	V+	0	*CG9381 (mura)*	CGd	2	1	*CG16788 (RnpS1)*	RB
C436 (2)	85D25	CD	0	*CG9399*	CGh	2	4	*CG8273*	RB
EP-686 (2)	85E14	F				1	1	*CG12418*	CG
C441 (1)	86F7	CD	1	*CG17342 (LK6)*	CS	1	NO		
C547 (1)	86F7	Bs	1	*CG31364 (l(3)neo38)*	CG	2	8	*CG14723 (HisCl1)*	CS
EP-650 (2)	87D9	V+	1	*CG12360*	CGh	2	0	*CG7620 (l(3)87Df)*	CGh
C18 (4)	87D9	CD	2	*CG8031*	CGh	2	0	*CG7583 (CtBP)*	TF
EP-1152.1 (2)	87E11	V+	0	*CG9764 (yrt)*	CY	1			
EP-149 (4)	88A4	B	0	*CG9924*	PP	2	0	*CG3050 (Cyp6d5)*	M
C840 (1)	88C6	V+	0	*CG7832*	CG	1			
EP-A7 (1)	88D1	bx	0	*CG7530*	CGh	1	NO		
EP-536 (1)	88D2	V+	0	*CG7425 (eff)*	PP	2	1	*CG3563*	CG
C875 (1)	88E1	B				0	NO		
EP-J76 (1)	88E3	CD	0	*CG6535 (tefu)*	CS	2	0	*CG4264 (Hsc70-4)*	PP
C278 (7)	88E4	V+	0	*CG6499*	M	2	3	*CG4285*	CG
EP-158 (1)	88F1	V−	1	*CG6202 (Surf4)*	CS	2	0	*CG31301*	TF
EP-767.1 (1)	89A8	V+	1	*CG18740 (mor)*	TF	2	4	*CG4261 (Hel89B)*	TF
C618 (10)	89B12	V+				1	0	*CG6889 (tara)*	TF
EP-207 (4)	89B12	V+, CD				1	0	*CG6963 (gish)*	CS
EP-167 (2)	89C7	V+	0	*CG14895 (Pak3)*	CS	1			
C607 (1)	89D5	F	1	*CG14905*	CGh	2	0	*CG6588 (Fas1)*	CA
EP-435 (2)	89E11	V−				1	0	*CG5201 (Dad)*	CS

(*continued*)

TABLE 1

(Continued)

P-GS line (no. insertions)	Citology	*shv*-Gal4	*D*	5′ gene	Molecular class	No. candidates	*D*	3′ gene	Molecular class
EP-87 (1)	89F3	V+				0	NO		
C923 (1)	90A3	B	1	*CG31256 (Brf)*	TF	2	0	*CG5851 (sds22)*	PPh
C819 (6)	90C1	V+	0	*CG7467 (osa)*	TF	1			
EP-36 (4)	92A1	V+	1	*CG3619 (Dl)*	CS	1			
C904.1 (3)	92B2	F	0	*CG4608 (bnl)*	CS	2	4	*CG31459*	CG
C246 (1)	92C1	B	0	*CG4413*	TF	2	1	*CG4936*	TF
C861 (1)	92F1	V+	2	*CG4241 (att-ORFA)*	M	2	1	*CG5180*	CG
EP-M68 (2)	92F1	V+				1	0	*CG5460 (H)*	CS, TF
EP-55 (4)	92F1	V+	0	*CG4257 (Stat92E)*	CS, TF	1			
C407 (3)	93B2	V+				1	0	*CG5670 (Atpalpha)*	M
EP-572 (1)	93B3	V−	1	*CG3593 (r-l)*	M	2	2	*CG5737 (dmrt93B)*	TF
C325 (1)	93C7	B	1	*CG3337*	CGh	2	0	*CG5874*	TF, RB
C211 (1)	93E9	F	0	*CG6376 (E2f)*	TF	1			
EP-J63.2 (1)	94E1	V−	0	*CG17894 (cnc)*	TF	1			
C279 (4)	94E1	V−	1	*CG4637 (hh)*	CS	1			
C411 (1)	94E9	CD	0	*CG4449*	PP	2	1	*CG6755*	TF, RB
EP-820 (1)	94E9	V+	4	*CG13825*	CG	2	3	*CG6755*	TF, RB
C588 (2)	94E9	wt	0	*CG10868 (orb)*	RB	2	1	*CG6759 (CDC16)*	PP
EP-111 (2)	94E9	V−	2	*CG17077 (pnt)*	CS, TF	2	2	*CG6768 (DNApol-epsilon)*	M
EP-654a (1)	95A7	Dif	NO			1	0	*CG10161 (eIF-3p66)*	RB
C933.1 (1)	95B1	V+	8/9	*CG33111/CG10192*	RB	3	1	*CR31185 (snRNA:U1:95Cc)*	snRNA
C919 (1)	95C5	F	0	*CG5320 (Gdh)*	M	1	NO		
C790 (1)	95D7	B	0/0	*CG5448 (Syx1A)/CG33110*	M/CG	3	2	*CG10694*	CGh
EP-51 (1)	96D4	wt	0	*CG4548 (XNP)*	TF	2	1	*CG5116*	CS
EP-469.1 (1)	96F10	V−	7	*CG6096 (m5)*	TF	2	1	*CG8361 (m7)*	TF
C442 (7)	98A2	V−	0	*CG5643 (wdb)*	PPh	2	1	*CG5692 (raps)*	CS
EP-298 (2)	98F1	B	3	*CG33203*	CG	2	0	*CG1658 (Doa)*	CS
C495 (1)	99D1	V−	1	*CG15525*	CGh	2	0	*CG11504*	CGd
C328 (1)	99E4	wt	2	*CG2216 (Fer1HCH)*	M	2	0	*CG1469 (Fer2LCH)*	M
EP-610 (1)	100B1	B	0	*CG1715 (l(3)03670)*	CGh	1	NO		
C166 (2)	100C7	CD	0	*CG11525 (CycG)*	CS	2	0	*CG1775 (Med)*	CS, TF
C345 (1)	100D2	CD	1	*CG2126*	CG	2	1	*CG1945 (faf)*	PP
C632 (2)	100D2	F	1	*CG2210 (awd)*	M	2	1	*CG1910*	CG
C705 (1)	102A3	F				1	0	*CG17964 (pan)*	TF
EP-241 (1)	102C1	B	0	*CG11533*	CS	1			
EP-140 (1)	102D1	CD	3	*CG11091 (sphinx)*	CG	1			

Each insertion site is represented by one P-GS line. Data are sorted by cytology. Phenotype in combination with *Gal4-shv*^{3Kpn} (*shv-Gal4*): thicker veins (V+), loss of veins (V−), defects in cell differentiation (CD), fails in dorso–ventral adhesion (B), defects in wing folding (F), alterations in polarity (Pol), defects in epithelial integrity (E), and wild type (wt). Molecular class: cell signaling (CS), transcription factor (TF), cell adhesion (CA), cytoskeleton (CY), metabolism (M), proteases (PP), RNA binding (RB), annotated genes with unknown function without homology (CG), those with homology (CGh), those with conserved structural domains (CGd), microRNA, snRNA, and tRNA. *D*, distance in kilobases of transcription initiation to the insertion site.

TABLE 2

Comparison of phenotypes observed in combinations between P-GS and UAS lines with two different Gal4 drivers

P-GS line	Gene 5′	Gene 3′	UAS line	Gal4-shv	Gal4-638
C279	CG4637 (hh)		UAS-hh	−L3	S-P
EP-36	CG3619 (Dl)		UAS-DI	+V	S-P
EP-E	CG9764 (yrt)		UAS-yrt	+V	S-P
EP-459		CG5201 (dad)	UAS-dad	−V	S-P
C107		CG6494 (h)	UAS-hairy	−V	−V
C192		CG7734 (shn)	UAS-shn	Bs	S-P
C166	CG11525 (CycG)	CG1775 (Med)	UAS-Med	CD	+V
C865	CG9181 (Ptp61F)	CG1214 (ru)	UAS-ru	+V	+V
EP-23	CG1429 (Mef2)	CG12130	UAS-Mef2	−V	N
EP-234	CG11617	CG11490	UAS-CG11617	−V	N
C517	CG9886	CG9885 (dpp)	UAS-dpp	+V	S-P
EP-704	CG10737	CG7097	UAS-CG7097	+V	N
EP-O	CG30184	CG5393 (apt)	UAS-apt	wt	S
EP-A	CG3653 (kirre)	CG3936 (N)	UAS-Notch	+V	+V

The P-GS lines analyzed (P-GS line), the adjacent genes to each P-GS insertion (5′ gene and 3′ gene), the corresponding UAS lines (UAS line), and the phenotypes observed in combinations between the P-GS insertion or its correspondent UAS construct with the Gal4 lines *Gal4-shv^{3Kpn}* and *Gal4-638* are shown. The different phenotypes are indicated as follows: ectopic or thicker veins (+V), loss of veins (−V), effects on wing size and pattern (S-P), cell differentiation (CD), blistered wings (Bs), and thickened L3 vein (+L3).

when the ectopic expression is induced in the wing disc (Figure 7, A and C, and Table 3). Similarly, effects restricted to the veins in combination with *638-Gal4* were rare for P-GS lines, causing wing blistering and folding phenotypes in combination with *Gal4-shv^{3Kpn}* (Figure 7, G and I). These two phenotypic classes also gave a high frequency of wild-type individuals in combinations with both *Gal4-253* and *Gal4-638* (Figure 7, G–J). There is also a high tendency for P-GS causing loss of veins in combination with *Gal4-shv^{3Kpn}* to eliminate the macrochaetae in combination with *Gal4-253* (Figure 7D). Finally, in combinations with *Gal4-638* the wing margin is affected in a high percentage of P-GS lines belonging to the "thick vein" phenotypic class (Figure 7A and Table 3). These two phenotypes, thick veins and loss of wing margin, are typical of a reduction in Notch signaling at different stages of development (Shellenbarger and Mohler 1978).

Molecular classes identified in the screen: The molecular mapping of the P-GS insertion sites allows a preliminary molecular annotation of the candidate genes to mediate the observed phenotypes. On the basis of the data presented in Table 2 and Figure 5, we believe that the phenotypes of *P-GS/Gal4* combinations are due in most cases to only one of the genes that are ectopically overexpressed. However, taking a parsimonious approach, we considered as candidates all genes positioned in a forward orientation whose 5′ region is within 10 kb of the insertion site. With these criteria, the number of candidate genes to mediate the mutant phenotypes is 373, of which 104 correspond to insertion sites with only one candidate gene, 248 correspond to insertion sites

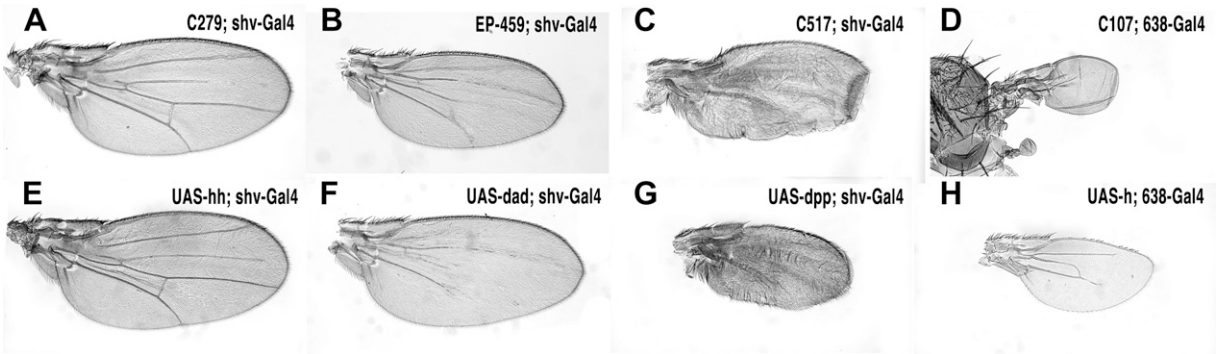

Figure 5.—Comparison between the phenotype of P-GS insertion and UAS constructs. (A–H) Representative examples of P-GS/Gal4 (A–D) and UAS/Gal4 (E–H) combinations. (A and E) Partial loss of L3 vein caused by ectopic expression of *hh* in pupal veins using the P-GS line *C279* (A) and *UAS-hh* (E). (B and F) Similar loss of vein differentiation caused by ectopic expression of *dad* in pupal veins using the P-GS line *EP-459* (B) and *UAS-dad* (F). (C and G) Differentiation of extra-vein tissue by ectopic expression of *dpp* in pupal veins using the P-GS line *C517* (C) and *UAS-dpp* (G). (D and H) Loss of veins and reduced wing size observed when *hairy* is expressed ectopically in the wing imaginal disc using the P-GS line *C107* (D) and *UAS-h* (H).

TABLE 3

Insertion sites grouped by phenotypic classes in combination with *Gal4-shv^{3Kpn}*, showing the phenotypes with *Gal4-638* and *Gal4-253*

P-GS	Cytology	638-Gal4	253-Gal4	5′ gene	3′ gene
			Vein thickening (*shv*-Gal4)		
C277	39B4	B	wt	*CG31626*	*CG8676 (Hr39)*
EP-720	22C1	F	wt	*CG15378 (lectin-22C)*	*CG4244 (su(dx))*
EP-232	29C3	F	wt	*CG13398*	*CG13388 (Akap200)*
C488	30F5	L	+Mq		*CG4722 (bib)*
C434.2	44C4	L	−Mq		
C7	49A4	L	wt	*CG8834*	*CG8525*
C708	67C7	N	+Mq	*CG6767*	*CG8284 (UbcD4)*
C717	30B5	N	−Mq	*CG4405 (jp)*	*CG3838*
C327.2	57E5	N	wt	*CG9847 (Fkbp13)*	*CG15669 (Mesk2)*
C767	62A1	N	wt	*CG13916*	
C343	85D21	N	wt	*CG9375 (Ras85D)*	*CG8161 (Rlb1)*
EP-536	88D2	N	wt	*CG7425 (eff)*	*CG3563*
EP-773	55F6	N	wt	*CG15098*	*CG15083*
EP-471	21B2	Ns	+Mq		*CG18497 (spen)*
EP-990	50D1	Ns	+Mq		*CG8118 (mam)*
C278	88E4	Ns	+Mq	*CG6499*	*CG4285*
C76	9D2	Ns	+Mq	*CG15302 (or9a)*	*CG15304*
EP-207	89B12	Ns	+Mq		*CG6963 (gish)*
EP-108	30F4	Ns	−Mq	*CG5838 (Dref)*	*CG4651 (RpL13)*
EP-643	85D22	Ns	−Mq	*CG9381 (mura)*	*CG16788 (RnpS1)*
C861	92F1	Ns	−Mq	*CG4241 (att-ORFA)*	*CG5180*
EP-M	36C5	Ns	wt	*CG6667 (dl)*	*CG5050*
C474.1	77B4	Ns	wt	*CG5585*	*CG5605 (eRF1)*
EP-M68	92F1	Ns	wt		*CG5460 (H)*
C407	93B2	Ns	wt		*CG5670 (Atpalpha)*
C639.1	56C1	Nw	+Mq		*CG7097*
C618	89B12	Nw	−Mq		*CG6889 (tara)*
C877	36A2	Nw	wt	*CG4952 (dac)*	*CG4599 (Trp2)*
C155	4B2	Nw	wt	*CG3665 (Fas2)*	
EP-822	21D1	S	+Mq	*CG17941 (ds)*	
EP-730	67C9	S	wt	*CG6721 (Gap1)*	
C858	8B4	S	wt	*CG10701 (Moe)*	
EP-24	29A1	S-P	+/−Mq	*CG8049 (Btk29A)*	
C517	22F2	S-P	+Mq		*CG9885 (dpp)*
C933.1	95B1	S-P	+Mq	*CG33111/CG10192*	*CR31185 (snRNA:U1:95Cc)*
C676	22E1	S-P	−Mq	*CG3664 (Rab5)*	*CG4272*
C478	50C14	S-P	−Mq	*CG6671 (AGO1)*	*CG33155/CG30481 (mRpL53)*
EP-575	58E4	S-P	−Mq	*CG4444 (px)*	
EP-820	94E9	S-P	−Mq	*CG13825*	*CG6755*
EP-284	60E1	S-P	wt	*CG16932 (Eps15)*	*CG3594 (Eap)*
EP-650	87D9	S-P	wt	*CG12360*	*CG7620 (l(3)87Df)*
EP-1152.1	87E11	S-P	wt	*CG9764 (yrt)*	
EP-167	89C7	S-P	wt	*CG14895 (Pak3)*	
EP-36	92A1	S-P	wt	*CG3619 (Dl)*	
C427	73D1	S-P	−Mq	*CG9668 (Rh4)*	*CG11914 (Lmpt)*
EP-767.1	89A8	V−	wt	*CG18740 (mor)*	*CG4261 (Hel89B)*
C31	21C2	V−(d)	−Mq	*CG11907 (Ent1)*	
C819	90C1	V+	wt	*CG7467 (osa)*	
EP-A	3C7	V+	−Mq		*CG3936 (N)*
C840	88C6	V+	−Mq	*CG7832*	
EP-55	92F1	V+	−Mq	*CG4257 (Stat92E)*	
EP-Z	10C9	V+	wt	*CG1697 (rho-4)*	
EP-1008	34D4	V+	wt		*CG7793 (Sos)*
EP-880	61C3	V+	wt	*CG13892 (Cypl)*	*CG17090*
C865	61F7	V+	wt	*CG9181 (Ptp61F)*	*CG1214 (ru)*
EP-M32	33B3	V+	wt	*CR31863 (bft)*	

(*continued*)

TABLE 3

(Continued)

P-GS	Cytology	638-Gal4	253-Gal4	5′ gene	3′ gene
EP-1	65C3	V+	wt	*CG10107*	*CG8549*
C909	69A4	V+	wt	*CG4300*	*CG10426*
EP-87	89F3	V+	wt		
EP-165	9E1	V+, B	wt	*CG32676*	*CG1799 (ras)*
EP-600	28D1	V+, Ns	+Mq		*CG7123 (LanB1)*
EP-489	3C6	wt	−Mq		*CG3653 (kirre)*
C356	46D7	wt	wt	*CG18445*	*CG2249*
C459	53F9	wt	wt	*CG8938 (GstS1)*	*CG30456*
EP-709	56F8	wt	wt		*CG8896 (18w)*
EP-644	60E5	wt	wt		*CG9071 (NaCP60E)*
EP-297.2	68F1	wt	wt	*CG12277 (rols)*	
			Loss of veins (*shv*-Gal4)		
C500	63C1	E	+/−Mq	*CG12078*	*CR33598 (mir-282)*
EP-469.2	5B5	N	+Mq	*CG3171 (Tre1)*	*CG15779 (Tre)*
EP-234	21B4	Ns	−Mq	*CG11617*	
EP-23	46C4	Ns	−Mq	*CG1429 (Mef2)*	
EP-J63.2	94E1	Ns	wt	*CG17894 (cnc)*	
EP-M89	45C3	Ns, E	−Mq	*CG2072 (TXBP181-like)*	*CG1975 (Rep2)*
EP-435	89E11	S-P	+/−Mq		*CG5201 (Dad)*
EP-(19)	32E2	S-P	−Mq	*CG6392 (cmet)*	*CG32955 (Cana)*
EP-572	93B3	S-P	−Mq	*CG3593 (r-l)*	*CG5737 (dmrt93B)*
C736	13F17	S-P	−Mq	*CG9056*	
EP-323	37B11	S-P	−Mq	*CG15173*	*CG10473*
EP-111	94E9	S-P	−Mq	*CG17077 (pnt)*	*CG6768 (DNApol-epsilon)*
EP-160	75F6	S-P	−Mq	*CG14080 (Mkp3)*	
C279	94E1	S-P	wt	*CG4637 (hh)*	
C442	98A2	S-P, E	+/−Mq	*CG5643 (wdb)*	*CG5692 (raps)*
EP-1152.2	59B6	S-P, E	−Mq	*CG3820 (Nup214)*	
EP-439	57F10	S-P, E	−Mq	*CG30404*	*CG17952*
EP-3	44C2	V−	L	*CG3161 (dpn)*	
C518	56E3	V−	−Mq	*CG9854 (hrg)*	*CG11025 (IsoT-3)*
EP-469.1	96F10	V−	−Mq	*CG6096 (m5)*	*CG8361 (m7)*
EP-708	60D9	V−	−Mq	*CG13594*	*CG3616 (Cyp9c1)*
EP-256	85C1	V−	−Mq	*CG11988 (neur)*	
EP-339	35E2	V−	−Mq	*CG4993 (PrL-1)*	*CG4930*
C17	35F1	V−	−Mq	*CG7664 (crp)*	*CG4132 (pkaap)*
EP-63	3A1	V−	wt	*CG14049 (Ilp6)*	*CG2845 (phl)*
EP-501	72D6	V−	wt	*CG5215 (Zn72D)*	*CG5444 (Taf4)*
C747	72F1	V−	wt	*CG4531 (argos)*	
C495	99D1	V−	wt	*CG15525*	*CG11504*
EP-899	28D3	V−	wt	*CG7233 (snoN)*	
C762	33F4	V−	wt	*CG12283 (kek-1)*	
EP-17	83A5	V−	wt	*CG2899 (ksr)*	*CG31550*
C926	85D1	V−	wt	*CG9746*	
EP-112	31A1	V−, N	−Mq		*CG4799 (Pen)*
EP-1013	70E5	V−, Nw	wt	*CG4879 (RecQ5)*	*CG5031 (dlp)*
C107	66D9	V−, S	−Mq		*CG6494 (hairy)*
EP-158	88F1	V+	wt	*CG6202 (Surf4)*	*CG31301*
EP-65	45F1	wt	wt	*CG1888*	*CR33010 (mir-14)*
			Cell differentiation (*shv*-Gal4)		
EP-405	44E3	B	+/−Mq	*CG8739 (cmp44E)*	*CG8740*
C125	60C7	F	wt	*CG4527 (Plkk1)*	*CG3416 (Mov34)*
C436	85D25	F	wt	*CG9399*	*CG8273*
C345	100D2	L	−Mq	*CG2126*	*CG1945 (faf)*
C255	66B3	L	−Mq	*CG7574 (bip1)/CR32358*	*CG13681*
C367	55B7	L	−Mq	*CG5753 (stau)*	*CG12767 (Dip3)*

(*continued*)

TABLE 3

(Continued)

P-GS	Cytology	638-Gal4	253-Gal4	5′ gene	3′ gene
C79	53F1	L	wt		*CG9635 (RhoGEF2)*
C432	67C4	L	wt	*CG6757 (SH3PX1)*	*CG16707 (vsg)*
C18	87D9	L	wt	*CG8031*	*CG7583 (CtBP)*
EP-67	21C6	L	wt		
EP-687	54F1	N	−Mq	*olf186-M*	*CG11430 (olf186-F)*
EP-319	42A4	N	−Mq	*CG12051 (Act42A)*	*CG7865 (PNGase)*
C606	85C4	N	−Mq	*CG9755 (Pum)*	
EP-476	32F2	N	wt	*CG31705*	
EP-634.2	57E8	N, V−	−Mq	*CG10496*	*CG15669 (Mesk2)*
C623	37D7	N, V−	wt	*CG10334 (spi)*	
EP-596	58F4	Ns	L	*CG30217*	*CG4250*
EP-J59	55B8	Ns	−Mq	*CG5748 (Hsf)*	*CG5119 (pAbp)*
C480	21C6	Ns	wt	*CG4427 (cabut)*	
C388	30B8	S	−Mq	*CG4422 (Gdi)*	
EP-450	62A3	S	wt	*CG12086 (cue)*	*CG1009 (Psa)*
EP-620	4E2	S-P	L	*CG32767*	
C603	51F11	S-P	−Mq	*CG8171 (dup)*	*CG8174 (SRPK)*
C293	61B3	S-P	−Mq	*CG7008 (Tudor-SN)*	*CG13880 (mRpL17)*
EP-140	102D1	S-P	wt	*CG11091 (sphinx)*	
EP-631	16C1	S-P	wt	*CG32556*	*CG5884 (par-6)*
C719.2	9F5	S-P	wt	*CG1655*	*CG2186*
C275	64E5	S-P, E		*CG10578 (DnaJ-1)*	*CG5486 (Ubp64E)*
EP-472	26A1	sW	−Mq	*CG9021*	*CG14001 (bchs)*
EP-689	12E5	sW	wt		*CG12047 (mud)*
C935	44F7	sW	wt	*CG8248*	*CG8243*
C411	94E9	sW	wt	*CG4449*	*CG6755*
EP-1052	9F5	sW	wt	*CG11207 (feo)*	*CG2186*
EP-603	27F1	V−	−Mq		*CG5261*
C174	26A5	V−	wt	*CG9553 (chic)*	*CG9075 (eIF-4a)*
C143	35D2	V−, S	−Mq	*CG3758 (esg)*	
EP-M71	27F3	V+	+V		*CG4971 (Wnt10)*
C166	100C7	V+	wt	*CG11525 (CycG)*	*CG1775 (Med)*
C545	66C11	V+, B	wt	*CG7163 (mkg-p)*	*CG13667*
C375	15C4	V+d	−Mq	*CG9089 (wus)*	
C839	47C1	wt	+Mq	*CG12342*	*CG12323 (Pros b5)*
C389	57A7	wt	−Mq	*CR33617 (mir-313)*	*CG13425 (bl)*
C441	86F7	wt	wt	*CG17342 (LK6)*	
EP-J76	88E3	wt	wt	*CG6535 (tefu)*	*CG4264 (Hsc70-4)*
C386	26B2	wt	wt	*CG9088 (lid)*	*CG9093 (Tsp26A)*
EP-731	31E1	wt	wt	*CG5355*	*CG5300 (Klp31E)*
EP-654a	95A7	wt	wt		*CG10161 (eIF-3p66)*
EP-380	67D2	wt	wt	*CG6674*	*CG11989 (Ard1)*
EP-947	57C4	wt	wt	*CG30389*	
EP-694	11A11	wt	wt	*CG1900 (Rab40)*	*CG17788*
			Blistered wings (*shv*-Gal4)		
EP-64	36A2	B	+Mq	*CG5953*	
EP-493	15F4	B	wt	*CG8915 (helicasa)*	*CG12996*
EP-500.2	24A1	B	wt	*CG10033 (for)*	
EP-P	76D1	B	wt	*CG8742 (Gyc76C)*	*CG8522 (HlH106)*
EP-J17b	70B1	B	wt	*CG10133*	
EP-614	56F16	B, S, E	wt	*CG13868*	*CG8920*
EP-179	32E1	L	+/−Mq	*CG4807 (ab)*	
C923	90A3	L	+Mq	*CG31256 (Brf)*	*CG5851 (sds22)*
C167	78B1	L	−Mq	*CG10564 (Ac78C)*	*CG32435 (chb)*
C246	92C1	L	−Mq	*CG4413*	*CG4936*
C800	17A8	L	wt		*CG6103 (CrebB-17A)*
C282	30C7	L	wt		*CG3998 (zf30c)*

(*continued*)

TABLE 3

(Continued)

P-GS	Cytology	638-Gal4	253-Gal4	5′ gene	3′ gene
C403	67B5	N	+Mq	*CG3445 (phol)*	*CG3552*
C359	38F1	N	−Mq		*CCG31673*
C684	7C4	N	wt	*CG10778*	*CG1524 (RpS14a)*
C37	24C3	Ns	+/−Mq		*CG10021 (bowl)*
EP-Ib	33A1	Ns, E	wt	*CG14938 (crol)*	
C790	95D7	Nw	+Mq	*CG5448 (Syx1A)/CG33110*	*CG10694*
C373	13F1	nW	−Mq		*CG8544 (sd)*
C677	56A1	S	wt		*CG12758 (sano)*
C27	52F8	S	wt	*CG8448 (mrj)*	
EP-241	102C1	S-P	wt	*CG11533*	
EP-329	64A7	S-P	wt	*CG14995*	*CG14991*
C371	43B1	S-P	wt	*CG1708 (cos)*	*CG11107*
C192	47D7	S-P	wt	*CG7734 (shn)*	
C67	67F4	S-P, +Q	+Mq	*CG12296 (klu)*	
EP-610	100B1	S-P, E	−Mq	*CG1715 (l(3)03670)*	
EP-182	75B1	sW	+Mq		*CG8127 (Eip7B)*
C832	16C1	sW	wt	*CG32556*	
C756	68B1	sW	wt	*CG6190*	*CG7600*
C272	75D1	wt	+Mq	*CG13702 (AlCR2)*	
C752	76D3	wt	+Mq	*CG8103 (Mi-2)/CG32217*	*CG7757*
C547	86F7	wt	−Mq	*CG31364 (l(3)neo38)*	*CG14723 (HisCl1)*
EP-149	88A4	wt	wt	*CG9924*	*CG3050 (Cyp6d5)*
C649	1E3	wt	wt		
C544	25B1	wt	wt		*CG3036*
EP-787	25C1	wt	wt	*CG8680*	
C719.1	38E3	wt	wt	*CG9318*	*CG2637 (Fs(2)Ket)*
C596	57E5	wt	wt	*CG10497 (Sdc)*	*CG15667 (sara)*
C875	88E1	wt	wt		
C325	93C7	wt	wt	*CG3337*	*CG5874*
C891	35A3	wt	wt	*CG4551 (smi35A)*	
EP-878	47A1	wt	wt	*CG3298 (JHI-1)*	*CG12909*
EP-298	98F1	wt	wt	*CG33203*	*CG1658 (Doa)*
EP-457	12F4	wt	wt	*CG9533 (rut)*	*CG14411*
EP-429	61F6	wt	wt	*CG2211*	*CG9165*
			Folded wing (*shv*-Gal4)		
C904.1	92B2	B	wt	*CG4608 (bnl)*	*CG31459*
C446	26B3	B	wt	*CG9154*	*CG9159 (Kr-h2)*
C109	42E4	F	wt	*CG3572 (vimar)*	*CG18742 (Tsp42Ea)/CG30159*
EP-872	69F4	F	wt		*CG11278 (Syntaxin13)*
C632	100D2	F	wt	*CG2210 (awd)*	*CG1910*
EP-686	85E14	F	wt		*CG12418*
C56	50E6	L	−Mq	*CG8542 (Hsc70-5)*	*CG8531*
C504	42E1	N	wt	*CG3572 (vimar)/CG30156*	*CG17002*
C211	93E9	Ns	+Mq	*CG6376 (E2f)*	
EP-800	25B3	Ns	−Mq	*CG8890 (Gmd)*	
C573	42E5	Ns	−Mq	*CG12846 (Tsp42Ed)*	*CG10106 (Tsp42Ee)*
C153	74D2	Ns	wt	*CG6311*	*CG7555 (Nedd4)*
C503	29C3	Ns	wt	*CG13398*	*CG13388 (Akap200)*
C549	64D1	nW	wt		
EP-B5	4C4	S-P	+/−Mq		*CG3578 (omb)*
C705	102A3	S-P	−Mq		*CG17964 (pan)*
C38	66A13	S-P	−Mq	*CG17888 (Pdp1)*	
EP-666	73D1	S-P	−Mq		*CG9712 (TSG101)*
EP-322	25B10	S-P, E	−Mq	*CG33113 (Rtnl1)*	
EP-608	51E3	S-P, V−, +Q	+Mq		*CG11798 (chn)*
C607	89D5	sW	wt	*CG14905*	*CG6588 (Fas1)*
C170	48A2	V+	wt	*CG10897 (tou)*	

(*continued*)

TABLE 3

(Continued)

P-GS	Cytology	638-Gal4	253-Gal4	5′ gene	3′ gene
C242	32B1	wt	−Mq	*CG6647 (porin)*	*CG17085*
C575	25B9	wt	wt	*CG8892*	*CG31653*
C207	52A8	wt	wt	*CG8183 (Khc-73)*	*CG30471*
EP-332	11D1	wt	wt	*CG33651*	
C919	95C5	wt	wt	*CG5320 (Gdh)*	

Phenotypic classes with *Gal4-638* (638-Gal4): thicker veins (V+), loss of veins (V−), moderate loss of wing margin (N), strong loss of wing margin (Ns), weak loss of wing margin (Nw), reduced wing size (S), reduced wing size with defects in vein patterning (S-P), defects in dorso–ventral adhesion (B), defects in wing expansion (F), defects in epithelial integrity (E), lethal (L), and wild type (wt). Phenotypic classes with *Gal4-253* (253-Gal4): extra bristles (+Mq), loss of bristles (−Mq), and wild type (wt).

with two candidate genes, and 21 to insertion sites with three or more candidate genes. In six cases we could not find any annotated gene in the proximity of the P-GS insertion. Most likely the 131 insertion sites with two or more candidates have at least one gene included in the annotation as "candidate" without contributing to the phenotype. The more represented molecular classes are cell signaling molecules (83) and transcription factors (64), which together correspond to 41% of the total annotated genes. Other molecular classes represented in high frequency are CG genes without clear structural homologies, which correspond to 22% of annotated genes. The frequency with which each molecular class is represented among phenotypic groups is similar, although some differences are apparent. For example, 60% of the genes corresponding to P-GS insertions removing the veins in combination with *shv-Gal4*^{3Kpn} correspond to the molecular classes cell signaling and transcription factors. In contrast, the frequency of CG genes in this phenotypic group is only 6% (Figure 8). Other molecular categories, including cell adhesion, cytoskeleton, RNA-binding proteins, and protein phosphatases, are distributed in a similar manner, comparing different phenotypic classes (Figure 8).

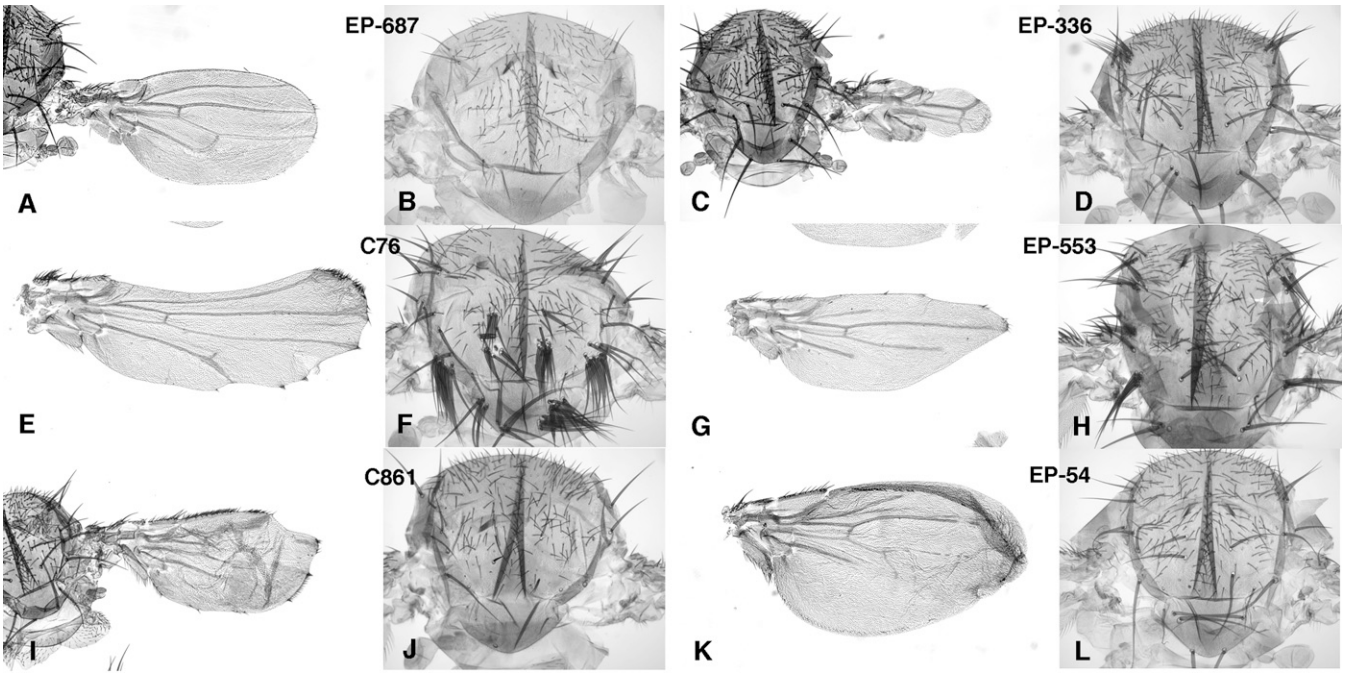

Figure 6.—Representative phenotypes observed in combinations between P-GS insertions and the Gal4 lines 638 and 253. The phenotypes in the wing (A, C, E, G, I, and K) in combinations with Gal4-638 and thorax (B, D, F, H, J, and L) in combinations with Gal4-253 of the P-GS insertions EP-687 (A and B), EP-336 (C and D), C76 (E and F), EP-553 (G and H), C861 (I and J), and EP-54 (K and L) are shown. The effects in the wing consist of loss of veins (A, G, and K), ectopic vein tissue (I), thickened veins (E), and loss of wing margin and associated wing tissue (A, C, E, G, and I). The phenotypes in the thorax are loss of macrochaetae (B, J, and L) and ectopic macrochaetae in clusters (D, F, and H).

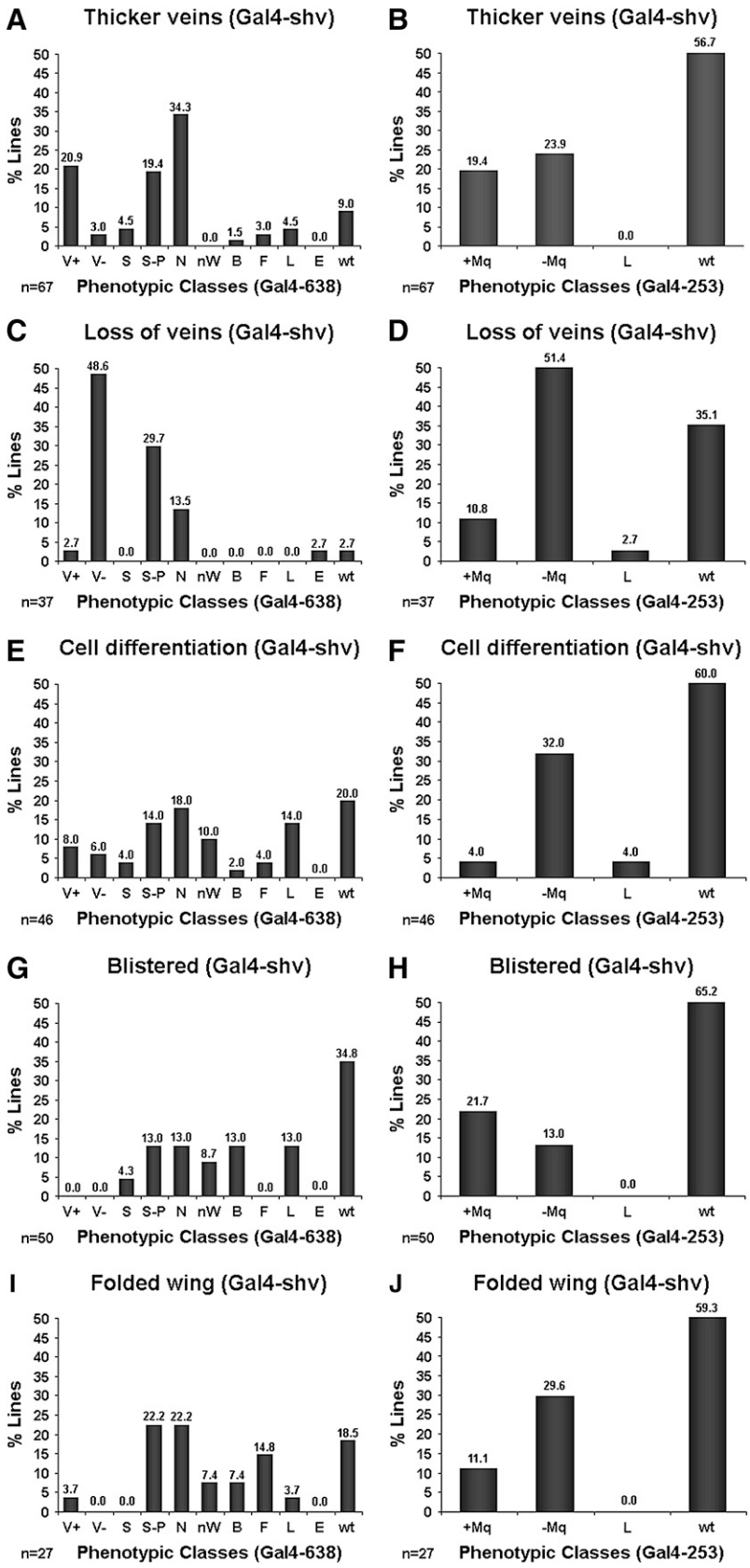

FIGURE 7.—Frequency of phenotypic classes obtained in combinations between the P-GS lines and the Gal4 lines *Gal4-638* (A, C, E, G, and I) and G*al4-253* (B, D, F, H, and J). The P-GS lines have been grouped after the phenotypes resulting in combinations with *Gal4-shv*^{3Kpn}: thicker veins (A and B), loss of veins (C and D), cell differentiation (E and F), blistered (G and H), and folded wing (I and J). (A–D) Most P-GS lines affecting the veins in combination with *Gal4-shv*^{3Kpn} also affect the veins when the ectopic expression is induced in the wing disc with *Gal4-638* (A and C). A high percentage of P-GS insertions causing thicker veins in combination with *Gal4-shv*^{3Kpn} also produce defects in the wing margin in combination with *Gal4-638*, whereas many P-GS insertions causing loss of veins in combination with *Gal4-shv*^{3Kpn} eliminate the macrochaetae in combination with *Gal4-253* (C and D, respectively). In contrast, many P-GS lines causing wing blistering and folded wing phenotypes in combination with *Gal4-shv*^{3Kpn} (G and I, respectively) result in wild-type phenotypes in combinations with both *Gal4-638* and *Gal4-253* (H and J). Symbols: V+, ectopic or thicker veins; V−, loss of veins; S, reduced wing size; S-P, reduced wing size and altered vein pattern; N, notched wings; nW, absence of wing blade tissue; B, blistered wing; F, folded wing; L, larval or pupal lethal; E, epithelial integrity alterations; wt, normal wings and normal chaetae pattern; +Mq, extra-macrochaetae; −Mq, loss of macrochaetae.

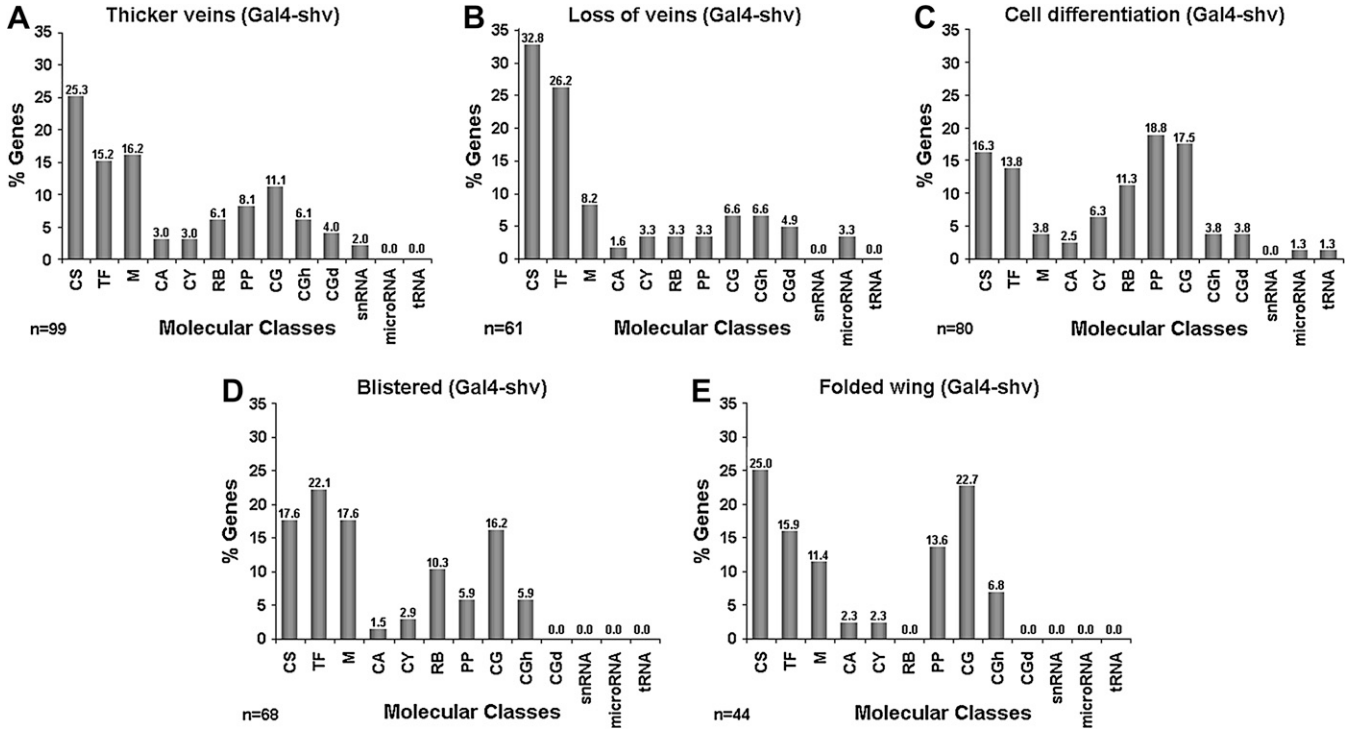

FIGURE 8.—Molecular classification of the genes identified grouped in the phenotypic classes obtained in combination with *Gal4-shv*: thicker veins (A), loss of veins (B), cell differentiation (C), blistered (D), and folded wing (E). The more represented molecular classes correspond to genes encoding proteins involved in cell signaling (CS) and transcription factors (TF), particularly for candidate genes causing loss of veins (B). Symbols: CS, signaling molecules; TF, transcription factors; M, metabolism; CA, cell adhesion; CY, cytosqueleton components; RB, RNA binding proteins; PP, protein proteases; CG, computer-annotated genes without identified structural domains; CGh, computer-annotated genes with vertebrate homologs; CGd, computer-annotated genes with a structural motive; snRNA, small nuclear RNA; microRNA, microRNA; tRNA, tRNA.

DISCUSSION

To identify genes regulating the formation of the Drosophila wing veins, we screened almost 13,000 new P-GS insertions in combination with a Gal4 driver expressed during the pupal development of the veins. We selected a collection of 500 P-GS insertions affecting the differentiation of the veins or the final steps of wing morphogenesis. These P-GS insertions were mapped by inverse PCR to the genomic sequence, identifying ~245 insertion sites. The frequency of P-GS insertions isolated corresponds to 4.17% of the 12,800 novel insertions screened, a result similar to other published EP screens. The viability and fertility of most *P-GS/shv-Gal4* combinations was a great advantage of this experiment, because it allowed carrying out the screen without the necessity of first establishing stocks of P-GS insertions. In practice, this permits screening a high number of insertions, by limiting the time-consuming task of generating and maintaining stocks to only those insertions selected by their effects on wing pattern. In this manner, we could overcome the limitation of other published screens using established EP collections that represent an estimated 10% of the 14,000 Drosophila annotated genes (RORTH *et al.* 1998).

Screen rationale: The basis of identifying genes by the consequences of their overexpression is that mutant phenotypes result from the expression of a gene in a place where it is not normally present (ectopic expression) and/or by its expression at higher than normal levels (gain-of-expression). We focused our analysis on the wing veins, because in their differentiation the Notch, EGFR, and Dpp pathways play a prominent role, by choosing a Gal4 line that is expressed only during the pupal development of the veins (SOTILLOS and DE CELIS 2006). In this way, the expression of Gal4 occurs after the wing disc cells proliferate and acquire their vein or intervein specifications in the disc (DE CELIS 2003). The restricted time window and tissue specificity of *Gal4-shv*^{3Kpn} expression implies that genes involved in vein differentiation, or able to interfere with the pupal development of the veins, are specifically targeted in the screen. We believe that the use of *Gal4-shv*^{3Kpn} should reduce the probability of isolating genes with pleiotropic overexpression effects unrelated to vein formation and, at the same time, increase the probability of identifying *bona fide* candidates to participate in vein formation. Furthermore, in the pupal veins there is a good correspondence between the loss-of-function phenotype and the alterations caused by ectopic expression

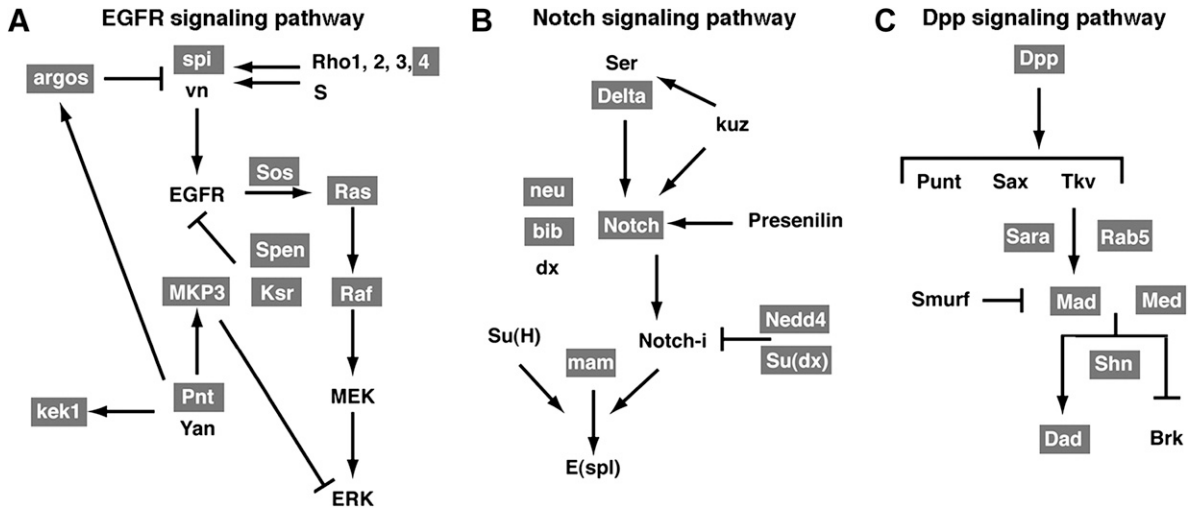

Figure 9.—Schematic of the core components belonging to the EGFR (A), Notch (B), and Dpp (C) signaling pathways. The relationships between different pathway members are indicated with arrows to denote activation or with bars to indicate repression. The genes included within shaded squares were identified in the screening as P-GS insertions close to their 5′ transcription start.

of known members of the signaling pathways regulating vein formation (Sotillos and De Celis 2005). Thus, reducing by mutation the activity of the Notch, EGFR, and Dpp signaling pathways causes opposite effects on vein formation than increasing the activity or expression of members of the corresponding pathways (see, for example, Figure 1). A large fraction of the P-GS isolated (46% of insertion sites) affected vein formation, and among them it is remarkable that we identify ~60% of the known genes belonging to the Notch, EGFR, and Dpp signaling pathways (Figure 9). This result illustrates the potential of the screen to identify additional components of these pathways, even though their actual involvement in vein formation must be determined by the analysis of loss-of-function phenotypes.

Limitations of the overexpression screen: There are several aspects of the presented screen that might limit its efficiency to identify a large fraction of the genes involved in vein pattern and wing morphogenesis. First, it is well known that *P* elements insert nonrandomly, with some sites highly preferred (hot spots) and others very rarely targeted by the *P* element (cold spots) (Liao *et al.* 2000). The *P*-element bias implies that only a fraction of genes will be targeted with a reasonable frequency to allow its identification in the screen. Thus, even though our starting collection was numerous, 12,800 new insertions, it is likely that many genes susceptible to affecting the veins when overexpressed were not targeted by P-GS insertions. In fact, the larger proportion of identified sites corresponds to unique insertions (60%), indicating that this screen is far from saturation. The second limitation of the screen is inherent to all searches based on a gain-of-expression phenotype, and it is related to the uncertainty about unspecific effects of ectopic expression on a particular developmental system. In several cases analyzed, where we could compare the loss- and gain-of-expression phenotypes of a given gene, we could find a correspondence between them. For example, overexpression of *Mkp3*, a phosphatase specific for the EGFR pathway member Rolled, causes the loss of veins, and the loss of *Mkp3* results in the differentiation of ectopic veins (Ruiz-Gomez *et al.* 2005). In some other cases, however, we observed that the loss- and gain-of-function phenotypes are not obviously related. Thus, ectopic expression of *LanB1* causes a vein thickening phenotype indistinguishable from that of the loss of Notch function, suggesting a functional relation between LanB1 activity and Notch signaling. However, the loss of *LanB1* in the wing causes the formation of wing blisters (C. Molnar and J. F. de Celis, unpublished results), a phenotype not obviously related to Notch activity. In this and other cases, it may happen that the relation of the considered gene to a particular pathway or network of interactions is limited to developmental processes distinct to vein formation, and only a careful analysis of the loss-of-function phenotype in other developmental processes might validate the functional inference made from adult phenotypes. Finally, not all genes required for vein formation previously characterized result in a mutant phenotype when overexpressed in the pupal veins (J. F. de Celis, unpublished results), limiting the subset of genes susceptible to be identified. With all these caveats in mind, we believe that the results of the screen include a large number of candidates that might prove instrumental to broaden our understanding of vein patterning and wing morphogenesis.

Developmental specificity of the novel P-GS insertions: The fact that vein formation is controlled by signaling pathways and transcription factors with

requirements in other developmental processes, such as imaginal disc growth and patterning, implies that many of the newly identified P-GS insertions should display phenotypes in combination with other Gal4 lines. This is indeed what we observed when the genes affected by the P-GS insertions were overexpressed in the wing blade or the proneural clusters. Thus, 86 and 53% of selected P-GS lines show a phenotype in combination with the drivers *Gal4-638* and *Gal4-253*, respectively (see Table 3). Similarly, we obtained a mutant phenotype in 87% of combinations with *Gal4-dll* and 57% of the combinations with *Gal4-ey*. The phenotypes in the leg (*Gal4-dll*) consist of the fusion of adjacent segments, the loss of distal tarsal segments, and pattern disorganization. These phenotypes are also observed upon interference with the Notch and EGFR signaling pathways (de Celis *et al.* 1998; Galindo *et al.* 2002). In the combinations with *ey-Gal4*, the most frequent alterations were reductions or absence of the eye, phenotypes also observed when Notch activity is reduced before ommatidial recruitment (Dominguez and de Celis 1998). In general, and for each P-GS insertion analyzed, there was good agreement between the phenotypes obtained by overexpression in different imaginal discs. Thus, by comparing these phenotypes to those obtained using UAS lines of known elements of the Notch, EGFR, and Dpp pathways, many P-GS lines can be tentatively ascribed to individual pathways. Therefore, although the driver used to select P-GS insertions is expressed only in the pupal wing veins, most genes affected by overexpression are required in other developmental processes controlled by similar networks of interactions.

Gene annotation of P-GS insertions: The use of the P-GS element in combination with several Gal4 lines results in a higher frequency of mutant phenotypes than the same combinations using other P-UAS elements (Toba *et al.* 1999). The ability of the P-GS to target genes localized at both ends of the insertion site increases the number of insertions with an overexpression phenotype, but complicates the assignment of the individual gene responsible for this phenotype. Thus, in all cases analyzed where two genes were present in the outward orientation with respect to the P-GS, we observed efficient transcription of both genes. By carrying out *in situ* hybridization in two clusters of genes targeted by several P-GS insertions we could define some rules that help in the annotation of the candidate genes. Thus, we did not observe transcription of antisense RNAs, suggesting that most phenotypes are due to the overexpression of genes in their normal transcriptional orientation. In addition, we find transcription in the Gal4 pattern of expression of genes separated from the P-GS insertion site by other coding regions. In one case we also observed Gal4/UAS-mediated transcription of two adjacent genes located at one end of the P-GS insertion site. In all cases analyzed, as expected, the level of ectopic expression was much higher than that of the endogenous expression of the gene, although no attempt was made to quantify the amount of ectopic expression. Thus, although our *in situ* data are limited to only a few cases, it seems clear that the efficiency of P-GS insertions to drive expression of adjacent genes varies depending on their genomic localization. Because there are no criteria *a priori* to discard adjacent genes as candidates on the basis of their molecular identity, we decided to incorporate in the annotation, presented in Table 1 and Figure 8, all genes oriented outwardly with respect to the P-GS insertion site and located within 10 kb from this site. By using these criteria, ~52% of insertion sites have two candidate genes to contribute to the gain-of-expression phenotype. We are aware that by these criteria many genes included in our annotation are not related to the corresponding overexpression phenotype, even though they will be overexpressed. Furthermore, in the cases that we were able to analyze in more detail, we could unambiguously ascribe the phenotype to only one of the annotated candidate genes. Thus, in 21 cases where two candidates fulfilled our criteria, and on the basis of the use of individual UAS lines, coexpression of interference RNA, or mapping of chemical revertants, the phenotype is caused by only one of the overexpressed genes. We expect this to be the case for a majority of P-GS insertions, although some cases with more than one gene contributing to the phenotype are also expected.

Molecular classes identified: The genes included in our annotation as candidates include a representation of most molecular categories, as well as a large number of computer-generated (CG) genes without significant structural homology to be included in a gene ontology (GO) class. Interestingly, the proportion of identified genes belonging to each GO class is very different from these frequencies in the Drosophila genome. For example, the fraction of CG genes with unknown function in the Drosophila genome is ~63% (Adams *et al.* 2000), and the same genes constitute between 18 and 28% of those identified in the screen. In contrast, the fraction of transcription factors in the Drosophila genome is 7% (Adams *et al.* 2000), and these genes constitute between 14 and 26% of the screen candidates. A similar difference is observed in the cell signaling class, with 10% in the genome (Adams *et al.* 2000) and between 16 and 32% of the screen candidates. These data indicate that the genes identified in the screen are not a random sample of the genome, because individual molecular classes are either under- or overrepresented. For the genes affecting the veins, the main objective of our screen, the two molecular classes most represented were signaling molecules and transcription factors. Most of these genes, as expected, also showed gain-of-expression phenotypes in other imaginal discs, implying a broad requirement during cell proliferation, pattern formation, and vein differentiation. We also found a number of genes whose possible implication in

a particular signaling pathway was not anticipated by previous functional assays. For example, the genes causing phenotypes reminiscent of loss-of-Notch signaling in different imaginal discs include *LanB1*, *Tre*, *yurt*, *ATPalpha*, and *CG6499*, and to our knowledge none of them have been previously related to Notch signaling. In all these cases the putative relationship to Notch signaling needs to be further established by the analysis of loss-of-function mutations. The possibility of generating small genetic deficiencies using the available collections of *P* and Hobo elements (Huet *et al.* 2002), the use of interference RNA, as well as the feasibility of isolating loss-of-function alleles as revertants of the original P-GS phenotype, would be invaluable in the functional analysis of these newly identified genes.

We are very grateful to A. García-Bellido for his continuous support and R. Barrio and Ed Ryder for their generous help in the early stages of this project. E. Sanchez-Herrero and A. Baonza are acknowledged for critical reading of the manuscript. Grants from Dirección General de Investigación Científica y Técnica BCM2003-01787 and GEN2001-4846-C05-01 to J.F.d.C. and an institutional grant from Fundación Ramón Areces to the Centro de Biología Molecular "Severo Ochoa" are also acknowledged.

LITERATURE CITED

Abdelilah-Seyfried, S., Y. M. Chan, C. Zeng, N. J. Justice, S. Younger-Shepherd *et al.*, 2000 A gain-of-function screen for genes that affect the development of the Drosophila adult external sensory organ. Genetics **155:** 733–752.

Adams, M. D., S. E. Celniker, R. A. Holt, C. A. Evans, J. D. Gocayne *et al.*, 2000 The genome sequence of Drosophila melanogaster. Science **287:** 2185–2195.

Adler, P. N., 2002 Planar signaling and morphogenesis in Drosophila. Dev. Cell **2:** 525–535.

Babcock, M. C., R. S. Stowers, J. Leither, C. S. Goodman and L. J. Pallanck, 2003 A genetic screen for synaptic transmission mutants mapping to the right arm of chromosome 3 in Drosophila. Genetics **165:** 171–183.

Bier, E., 2000 Drawing lines in the Drosophila wing: initiation of wing vein development. Curr. Opin. Genet. Dev. **10:** 393–398.

Bloor, J. W., and N. H. Brown, 1998 Genetic analysis of the Drosophila alphaPS2 integrin subunit reveals discrete adhesive, morphogenetic and sarcomeric functions. Genetics **148:** 1127–1142.

Bour, B. A., M. A. O'Brien, W. L. Lockwood, E. S. Goldstein, R. Bodmer *et al.*, 1995 Drosophila MEF2, a transcription factor that is essential for myogenesis. Genes Dev. **9:** 730–741.

Brand, A. H., and N. Perrimon, 1993 Targeted gene expression as a means of altering cell fates and generating dominant phenotypes. Development **118:** 401–415.

Brumby, A., J. Secombe, J. Horsfield, M. Coombe, N. Amin *et al.*, 2004 A genetic screen for dominant modifiers of a cyclin E hypomorphic mutation identifies novel regulators of S-phase entry in Drosophila. Genetics **168:** 227–251.

Buff, E., A. Carmena, S. Gisselbrecht, F. Jimenez and A. Michelson, 1998 Signalling by the Drosophila epidermal growth factor receptor is required for the specification and diversification of embryonic muscle progenitors. Development **125:** 2075–2086.

de Celis, J. F., 1997 Expression and function of decapentaplegic and thick veins in the differentiation of the veins in the Drosophila wing. Development **124:** 1007–1018.

de Celis, J. F., 2003 Pattern formation in the Drosophila wing: the development of the veins. BioEssays **25:** 443–451.

de Celis, J. F., S. Bray and A. Garcia-Bellido, 1997 Notch signalling regulates *veinlet* expression and establishes boundaries between veins and interveins in the *Drosophila* wing. Development **124:** 1919–1928.

de Celis, J. F., D. M. Tyler, J. de Celis and S. J. Bray, 1998 Notch signalling mediates segmentation of the Drosophila leg. Development **125:** 4617–4626.

Diaz-Benjumea, F., and A. Garcia-Bellido, 1990 Genetic analysis of the wing vein pattern of Drosophila. Wilhelm Roux Arch. Dev. Biol. **198:** 336–354.

Dominguez, M., and J. F. de Celis, 1998 A dorsal/ventral boundary established by Notch controls growth and polarity in the Drosophila eye. Nature **396:** 276–278.

Eulenberg, K. G., and R. Schuh, 1997 The tracheae defective gene encodes a bZIP protein that controls tracheal cell movement during Drosophila embryogenesis. EMBO J. **16:** 7156–7165.

Galindo, M. I., S. A. Bishop, S. Greig and J. P. Couso, 2002 Leg patterning driven by proximal-distal interactions and EGFR signaling. Science **297:** 256–259.

Garcia-Bellido, A., and J. Dapena, 1974 Induction, detection and characterization of cell differentiation mutants in Drosophila. Mol. Gen. Genet. **128:** 117–130.

Gelbart, W. M., M. Crosby, B. Matthews, W. P. Rindone, J. Chillemi *et al.*, 1997 FlyBase: a Drosophila database. The FlyBase consortium. Nucleic Acids Res. **25:** 63–66.

Golic, K. G., 1991 Site-specific recombination between homologous chromosomes in *Drosophila*. Science **252:** 958–961.

Hall, L. E., S. J. Alexander, M. Chang, N. S. Woodling and B. Yedvobnick, 2004 An EP overexpression screen for genetic modifiers of Notch pathway function in Drosophila melanogaster. Genet. Res. **83:** 71–82.

Huet, F., J. T. Lu, K. V. Myrick, L. R. Baugh, M. A. Crosby *et al.*, 2002 A deletion-generator compound element allows deletion saturation analysis for genomewide phenotypic annotation. Proc. Natl. Acad. Sci. USA **99:** 9948–9953.

Huppert, S., T. Jacobsen and M. A. T. Muskavitch, 1997 Feedback regulation is central to Delta-Notch signalling required for Drosophila wing vein morphogenesis. Development **124:** 3283–3291.

Ingham, P. W., and M. J. Fietz, 1995 Quantitative effects of hedgehog and decapentaplegic activity on the patterning of the Drosophila wing. Curr. Biol. **5:** 432–440.

Ito, K., W. Awano, K. Suzuki, Y. Hiromi and D. Yamamoto, 1997 The *Drosophila* mushroom body is a quadruple structure of clonal units each of which contains a virtually identical set of neurones and glial cells. Development **124:** 761–771.

Janody, F., J. D. Lee, N. Jahren, D. J. Hazelett, A. Benlali *et al.*, 2004 A mosaic genetic screen reveals distinct roles for trithorax and polycomb group genes in Drosophila eye development. Genetics **166:** 187–200.

Kiger, Jr., J. A., J. E. Natzle and M. M. Green, 2001 Hemocytes are essential for wing maturation in Drosophila melanogaster. Proc. Natl. Acad. Sci. USA **98:** 10190–10195.

Kimura, K., A. Kodama, Y. Hayasaka and T. Ohta, 2004 Activation of the cAMP/PKA signaling pathway is required for post-ecdysial cell death in wing epidermal cells of Drosophila melanogaster. Development **131:** 1597–1606.

Kinchen, J. M., and M. O. Hengartner, 2005 Tales of cannibalism, suicide, and murder: programmed cell death in C. elegans. Curr. Top. Dev. Biol. **65:** 1–45.

Lawrence, N., T. Klein, K. Brennan and A. Martinez Arias, 2000 Structural requirements for Notch signalling with Delta and Serrate during the development and patterning of the wing disc of Drosophila. Development **127:** 3185–3195.

Liao, G. C., E. J. Rehm and G. M. Rubin, 2000 Insertion site preferences of the P transposable element in Drosophila melanogaster. Proc. Natl. Acad. Sci. USA **97:** 3347–3351.

Marquez, R. M., M. A. Singer, N. T. Takaesu, W. R. Waldrip, Y. Kraytsberg *et al.*, 2001 Transgenic analysis of the Smad family of TGF-β signal transducers in *Drosophila melanogaster* suggests new roles and new interactions between family members. Genetics **157:** 1639–1648.

Marty, T., B. Muller, K. Basler and M. Affolter, 2000 Schnurri mediates Dpp-dependent repression of brinker transcription. Nat. Cell Biol. **2:** 745–749.

Minami, M., N. Kinoshita, Y. Kamoshida, H. Tanimoto and T. Tabata, 1999 *brinker* is a target of Dpp in *Drosophila* that negatively regulates Dpp-dependent genes. Nature **398:** 242–246.

Nellen, D., R. Burke, G. Struhl and K. Basler, 1996 Direct and long range action of a DPP morphogen gradient. Cell **85:** 357–368.

Nusslein-Volhard, C., E. Wieschaus and H. Kluding, 1984 Mutations affecting the pattern of the larval cuticle in Drosophila melanogaster. Roux's Arch. Dev. Biol. **193:** 267–282.

Nybakken, K., S. A. Vokes, T. Y. Lin, A. P. McMahon and N. Perrimon, 2005 A genome-wide RNA interference screen in Drosophila melanogaster cells for new components of the Hh signaling pathway. Nat. Genet. **37:** 1323–1332.

Pena-Rangel, M. T., I. Rodriguez and J. R. Riesgo-Escovar, 2002 A misexpression study examining dorsal thorax formation in *Drosophila melanogaster*. Genetics **160:** 1035–1050.

Raymond, K., E. Bergeret, A. Avet-Rochex, R. Griffin-Shea and M. O. Fauvarque, 2004 A screen for modifiers of RacGAP(84C) gain-of-function in the Drosophila eye revealed the LIM kinase Cdi/TESK1 as a downstream effector of Rac1 during spermatogenesis. J. Cell Sci. **117:** 2777–2789.

Ripoll, P., and A. Garcia-Bellido, 1973 Cell autonomous lethals in Drosophila melanogaster. Nat. New Biol. **241:** 15–16.

Robertson, H. M., C. R. Preston, R. W. Phillis, D. M. Johnson-Schlitz, W. K. Benz *et al.*, 1988 A stable genomic source of *P*-element transposase in *Drosophila melanogaster*. Genetics **118:** 461–470.

Rorth, P., K. Szabo, A. Bailey, T. Laverty, J. Rehm *et al.*, 1998 Systematic gain-of-function genetics in Drosophila. Development **125:** 1049–1057.

Ruiz-Gomez, A., A. Lopez-Varea, C. Molnar, E. de la Calle-Mustienes, M. Ruiz-Gomez *et al.*, 2005 Conserved cross-interactions in Drosophila and Xenopus between Ras/MAPK signaling and the dual-specificity phosphatase MKP3. Dev. Dyn. **232:** 695–708.

Schulz, C., A. A. Kiger, S. I. Tazuke, Y. M. Yamashita, L. C. Pantalena-Filho *et al.*, 2004 A misexpression screen reveals effects of *bag-of-marbles* and TGFβ class signaling on the Drosophila male germline stem cell lineage. Genetics **167:** 707–723.

Schupbach, T., and E. Wieschaus, 1986 Germline autonomy of maternal-effect mutations altering the embryonic body pattern of Drosophila. Dev. Biol. **113:** 443–448.

Shellenbarger, D. L., and J. D. Mohler, 1978 Temperature-sensitive periods and autonomy of pleiotropic effects of l(1)Nts1, a conditional Notch lethal in Drosophila. Dev. Biol. **62:** 432–446.

Sotillos, S., and J. F. De Celis, 2005 Interactions between the Notch, EGFR, and decapentaplegic signaling pathways regulate vein differentiation during Drosophila pupal wing development. Dev. Dyn. **232:** 738–752.

Sotillos, S., and J. F. de Celis, 2006 Regulation of decapentaplegic expression in the pupal wing veins. Mech. Dev. **123:** 241–251.

Staehling-Hampton, K., and F. M. Hoffmann, 1994 Ectopic *decapentaplegic* in the *Drosophila* midgut alters the expression of five homeotic genes, *dpp*, and *wingless*, causing specific morphological defects. Dev. Biol. **164:** 502–512.

Tanimoto, H., S. Itoh, P. ten Dijke and T. Tabata, 2000 Hedgehog creates a gradient of DPP activity in Drosophila wing imaginal discs. Mol. Cell **5:** 59–71.

Toba, G., T. Ohsako, N. Miyata, T. Ohtsuka, K. H. Seong *et al.*, 1999 The gene search system. A method for efficient detection and rapid molecular identification of genes in *Drosophila melanogaster*. Genetics **151:** 725–737.

Tseng, A. S., and I. K. Hariharan, 2002 An overexpression screen in Drosophila for genes that restrict growth or cell-cycle progression in the developing eye. Genetics **162:** 229–243.

Tsuneizumi, K., T. Nakayama, Y. Kamoshida, T. Koernberg, J. Christian *et al.*, 1997 Daughters against dpp modulates dpp organizing activity in Drosophila wing development. Nature **389:** 627–631.

Verde, F., J. Mata and P. Nurse, 1995 Fission yeast cell morphogenesis: identification of new genes and analysis of their role during the cell cycle. J. Cell Biol. **131:** 1529–1538.

Walsh, E. P., and N. H. Brown, 1998 A screen to identify Drosophila genes required for integrin-mediated adhesion. Genetics **150:** 791–805.

Xu, T., and G. M. Rubin, 1993 Analysis of genetic mosaics in developing and adult Drosophila tissues. Development **117:** 1223–1237.

Zhu, M. Y., R. Wilson and M. Leptin, 2005 A screen for genes that influence fibroblast growth factor signal transduction in Drosophila. Genetics **170:** 767–777.

Zipperlen, P., K. Nairz, I. Rimann, K. Basler, E. Hafen *et al.*, 2005 A universal method for automated gene mapping. Genome Biol. **6:** R19.

Communicating editor: K. G. Golic